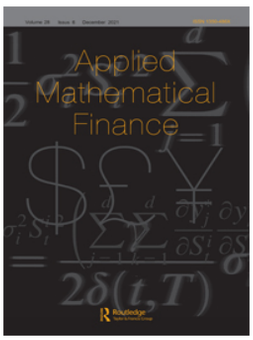

Routledge
Taylor & Francis Group

Applied Mathematical Finance

ISSN: (Print) (Online) Journal homepage: https://www.tandfonline.com/loi/ramf20

Expected Utility Theory on General Affine GARCH Models

Marcos Escobar-Anel, Ben Spies & Rudi Zagst

To cite this article: Marcos Escobar-Anel, Ben Spies & Rudi Zagst (2021) Expected Utility Theory on General Affine GARCH Models, Applied Mathematical Finance, 28:6, 477-507, DOI: 10.1080/1350486X.2022.2101010

To link to this article: https://doi.org/10.1080/1350486X.2022.2101010

Published online: 24 Jul 2022.

Submit your article to this journal

Article views: 37

View related articles

View Crossmark data

Full Terms & Conditions of access and use can be found at
https://www.tandfonline.com/action/journalInformation?journalCode=ramf20

APPLIED MATHEMATICAL FINANCE
2021, VOL. 28, NO. 6, 477–507
https://doi.org/10.1080/1350486X.2022.2101010

Routledge
Taylor & Francis Group

Check for updates

Expected Utility Theory on General Affine GARCH Models

Marcos Escobar-Anel [a], Ben Spies[b] and Rudi Zagst[b]

[a]Department of Statistical and Actuarial Sciences, University of Western Ontario, London, ON, Canada;
[b]Department of Mathematics, Technical University of Munich, Munich, Germany

ABSTRACT

Expected utility theory has produced abundant analytical results in continuous-time finance, but with very little success for discrete-time models. Assuming the underlying asset price follows a general affine GARCH model which allows for non-Gaussian innovations, our work produces an approximate closed-form recursive representation for the optimal strategy under a constant relative risk aversion (CRRA) utility function. We provide conditions for optimality and demonstrate that the optimal wealth is also an affine GARCH. In particular, we fully develop the application to the IG-GARCH model hence accommodating negatively skewed and leptokurtic asset returns. Relying on two popular daily parametric estimations, our numerical analyses give a first window into the impact of the interaction of heteroscedasticity, skewness and kurtosis on optimal portfolio solutions. We find that losses arising from following Gaussian (sub-optimal) strategies, or Merton's static solution, can be up to 2.5% and 5%, respectively, assuming low-risk aversion of the investor and using a five-years time horizon.

ARTICLE HISTORY
Received 30 November 2021
Accepted 7 July 2022

KEYWORDS
Dynamic portfolio optimization; affine GARCH models; non-Gaussian innovations; IG-GARCH model; expected utility theory; wealth-equivalent loss

1. Introduction

In times of extremely low-interest rates, the problem of optimal resource allocation is more relevant than ever. The idea of approaching this task in multiple discrete time steps via an optimization of expected utility derived from terminal wealth was first published by Mossin (1968) and subsequently extended by Samuelson (1969). While their approach was fairly general in terms of admissible probability distributions for the asset return, these returns were assumed to be i.i.d. and there was no recursive dynamics underlying. Merton (1969) transferred this approach to a continuous-time framework with a richer model, a geometric Brownian motion (GBM), developing closed-form solutions for utility functions of the CRRA type (*constant relative risk aversion*). His solution, due to its popularity, will play a major role in our paper, serving as a benchmark for the performance of our new strategy.

The simplicity of those models leads to the question of how to best describe the underlying price processes over time. After the hype on GBM in the seventies (Black and

CONTACT Marcos Escobar-Anel marcos.escobar@uwo.ca Department of Statistical and Actuarial Sciences, University of Western Ontario, London, ON N6A5B7, Canada

© 2022 Taylor & Francis

Scholes 1973; Merton 1973), more complex and realistic stochastic processes were introduced, for instance the stochastic volatility model in Heston (1993). This model was solved in the context of expected utility theory (EUT) in the early 2000s, e.g., Kraft (2005). Nonetheless, the models still bear difficulties with respect to implementation and testing originating from their continuous-time character. One possible answer consists of using discrete-time GARCH models, first introduced by Engle (1982) and Bollerslev (1986). Unfortunately, these usually do not yield closed-form solutions in the context of derivative pricing and portfolio optimization.

The lack of closed-form expressions for derivative pricing was overcome in Heston and Nandi (2000), introducing a GARCH model (referred to as the HN-GARCH) with Gaussian innovations, where the moment generating function (m.g.f.) of the log price process is available in exponentially affine form. This establishes a new class of so-called affine GARCH models. Several years later, Christoffersen, Heston, and Jacobs (2006) and Ornthanalai (2014) presented alternative affine GARCH models of non-Gaussian type, using Inverse-Gaussian and Lévy innovations, respectively, extending the range of accommodated stylized facts of asset returns. More recently, Badescu, Cui, and Ortega (2019) characterized the requirements for the above mentioned affine structure, demanding an exponentially affine form of the conditional bivariate cumulant generating function of the log asset price and its conditional variance. This guarantees a closed-form m.g.f. for option pricing formulas. The worlds of EUT and HN-GARCH model have been recently combined in Escobar-Anel, Gollart, and Zagst (2022); the authors relied on the log approximation of returns proposed by Campbell and Viceira (1999) to produce a first approximate closed-form solution to GARCH type models in dynamic portfolio optimization. Our paper extends their work by considering general affine GARCH processes as defined by Badescu, Cui, and Ortega (2019), with a focus on studying the implications of an IG-GARCH non-Gaussian setting.

Our contributions are the following:

- Assuming a CRRA utility function for the decision maker and the implied EUT setting of Campbell and Viceira (1999), we demonstrate that the optimal portfolio strategy in a general affine GARCH setting is available in recursive form, and the optimal wealth process is again an affine GARCH process.
- We demonstrate that a slight relaxation of the conditions on general affine GARCH models suffices to include the IG-GARCH model as a special case. This allows us to investigate the impact of negative skewness and leptokurtosis of asset returns on portfolio decisions.
- For two relevant parametric sets, we illustrate that the necessary adjustments on the portfolio due to the self-financing condition (SFC) approximation, i.e., the approximation proposed by Campbell and Viceira (1999), are negligible over the entire investment period.
- We expose, via the influence of the parameter η, that the more negative the skewness (and the higher the excess kurtosis), the lower the risky portfolio allocation – which could be of up to 50% less (low-risk aversion) than the allocation recommended by a Gaussian (HN-GARCH) framework. The market price of risk can also notably influence the optimal solution, the remaining parameters in the model have far less impact.

- The popular solution in the HN-GARCH context and Merton's static solution are used as suboptimal strategies to evaluate wealth-equivalent losses (WEL) compared to the optimal solution in our framework. The analysis reveals that the HN-GARCH strategy consistently outperforms Merton's solution for both parametric sets. Big changes in the higher moments of log asset return innovations can lead to high wealth-equivalent losses. For an investor with low-risk aversion, assuming a time horizon of five years, the WEL could be up to 2.5% of the initial wealth – using Merton's solution instead could even increase this number to 5%. In general, the WEL decreases with the level of risk aversion and it increases with the length of the time horizon.

The paper is organized as follows. In Section 2, the portfolio optimization problem to be tackled is defined and an outline of our solution approach is given. Subsequently, in Section 3, we present the optimal strategy in a general affine GARCH context as our main theoretical result and add a subsection about quantifying losses from following sub-optimal strategies. Section 4 applies the theoretical results to the IG-GARCH model, which is also the foundation for the numerical analyses in Section 5. In the latter part, we first investigate the feasibility of our solution, the impact of the used SFC approximation, and subsequently show the sensitivity of the optimal strategy with respect to the different IG-GARCH parameters. This is followed by an explicit comparison to the HN-GARCH solution, before we analyse the wealth-equivalent losses from following the Gaussian alternative or Merton's static solution. We conclude in Section 6.

2. Outline of the Approach

This section presents the general optimization framework for our investment problem and embeds general affine GARCH models in this context. We assume that the log price process $X_t = \log S_t$, the price at time t being S_t, follows an affine GARCH model (as defined by Badescu, Cui, and Ortega 2019), where for simplicity of exposition we assume $\Delta = 1$ for the length of the time step. Let θ be a vector of parameters and $\{\epsilon_t\}_{t=1,2,\dots}$ a sequence of $\mathcal{F}_t$-measurable and $\mathcal{F}_{t-1}$-conditional i.i.d. random variables with a finite moment generating function. Based on the associated filtered probability space $(\Omega, \mathcal{F}, \{\mathcal{F}_t\}_{t=0,1,\dots}, \mathbb{P})$ with physical measure $\mathbb{P}$, the model dynamics is:

$$Y_t := X_t - X_{t-1} = f_1(h_t, \theta) + \sqrt{h_t}\epsilon_t, \tag{1a}$$

$$h_{t+1} = f_2(h_t, \theta) + f_3(h_t, \epsilon_t, \theta), \tag{1b}$$

where f_1, f_2 are affine in h_t, while f_3 is such that the following representation for the conditional bivariate moment generating function holds:

$$\begin{aligned}\psi_{(X_t,h_{t+1})}(u, v|\mathcal{F}_{t-1}) &= \mathbb{E}\left[\exp\{u \cdot X_t + v \cdot h_{t+1}\}\middle|\mathcal{F}_{t-1}\right] \\ &= \exp\{uX_{t-1} + A(u, v; t-1, t) + B(u, v; t-1, t) \cdot h_t\}. \end{aligned} \tag{2}$$

The conditional expectation w.r.t. $\mathcal{F}_t$ will also be denoted via the subindex t, e.g., with $\mathbb{E}_t$, in the sequel. Note that the moment generating function in (2) can also be formulated for the log return instead of the log price as the first element, making the term uX_{t-1} in the exponential function vanish. The choice of f_1, f_2 and f_3 for a particular application shapes

the coefficients A and B in Equation (2) according to this requirement. The particular form of said coefficients will play a major role also in our framework.

We consider a portfolio optimization problem with finite time horizon T in a setting with one risky asset and the cash account B_t. For $t \in \{0, \dots T-1\}$, let π_t denote the fraction of wealth invested in the risky asset, let V_t be the corresponding wealth and $w_0 = \log v_0$ the log of the initial wealth. Following the reasoning in Escobar-Anel, Gollart, and Zagst (2022), we approximate returns in the self-financing condition by log prices. That is, we approximate the equation

$$\frac{V_t}{V_{t-1}} = \pi_{t-1}\frac{S_t}{S_{t-1}} + (1-\pi_{t-1})\,\mathrm{e}^r, \tag{3}$$

with r being the continuously compounded riskless rate, via a second-order Taylor approximation of the logarithm around 1, starting from $W_0 = w_0$. This leads to an approximation of the self-financing condition that reads:

$$W_t = W_{t-1} + \pi_{t-1}(X_t - X_{t-1}) + \tfrac{1}{2}\left(\pi_{t-1} - \pi_{t-1}^2\right) h_t + (1-\pi_{t-1})r. \tag{4}$$

This second-order approximation is well-studied – in particular, it corresponds to Equation (16) in Campbell and Viceira (1999). Equation (4) exactly equals (3) in the limit for $\Delta \to 0$, i.e., as the length of the trading interval approaches zero. We refer to Section 5.1 for an investigation of the quality of this approximation in our framework.

The goal is to maximize the expected utility from terminal wealth over the set of admissible, self-financing, relative portfolio strategies $\{\pi_t\}_{t=0}^{T-1}$. To this end, assume wealth is assessed by the decision maker according to a *power utility function* of the form $U(v) = (1/\gamma)v^\gamma$ for some parameter $\gamma < 1$, implying constant relative risk aversion (CRRA) $1-\gamma$. The stochastic control problem can be represented as follows:

$$\max_{\{\pi_t\}_{t=0}^{T-1}} \mathbb{E}\left[\frac{\exp\{\gamma W_T\}}{\gamma}\middle|\mathcal{F}_0\right] =: \phi_0\left(w_0, h_1\right), \tag{5}$$

where h denotes the conditional variance process of the log return of the underlying asset.

Let $\mathbb{A}$ be the set of admissible portfolios, $\mathbb{H} = (0,\infty)$ and $\mathbb{Y} = (0,\infty)$ be the domains of the conditional variance and the log return of the stock prices, respectively. Let $\mathbb{W} \subset \mathbb{R}$ be the set of possible values for the log wealth. Then, the transition function is given by $\mathbb{T} : \mathbb{W} \times \mathbb{A} \times \mathbb{H} \times \mathbb{Y} \to \mathbb{W} \times \mathbb{H}$,

$$\begin{aligned}\mathbb{T}(W, a, h, Y) := \Bigg(& W + aY + \frac{1}{2}\left(a - a^2\right)h + (1-a)r, \\ & f_2(h,\theta) + f_3\left(h, \frac{Y - f_1(h,\theta)}{\sqrt{h}}, \theta\right)\Bigg).\end{aligned} \tag{6}$$

Now assume that there exists a subset $\mathbb{M}$ of all integrable value functions $\phi : \mathbb{W} \times \mathbb{H} \to \mathbb{R}$ such that $\phi_T(W_T) = U(\exp\{W_T\}) \in \mathbb{M}$. With the operators $\mathbb{L}$ and $\mathbb{U}$,

$$\begin{aligned}\mathbb{L}\phi(W, a, h) &:= \mathbb{E}\left[\phi\left(\mathbb{T}(W, a, h, Y)\right)\right], \\ \mathbb{U}\phi(W, h) &:= \max_{a \in \mathbb{A}} \mathbb{L}\phi(W, a, h),\end{aligned}$$

assumed to be well-defined for all $\phi \in \mathbb{M}$, we moreover require for any $\phi \in \mathbb{M}$ the existence of some $a : \mathbb{W} \times \mathbb{H} \to \mathbb{A}$ with $a(W,h)$ maximizing $a \mapsto \mathbb{L}\phi(W,a,h)$ on $\mathbb{A}$ for all $W \in \mathbb{W}$ and $h \in \mathbb{H}$, and $\mathbb{U} : \mathbb{M} \to \mathbb{M}$.

Applying the main theorem for finite-step stochastic control models, we can make use of *Bellman's value iteration* and maximize recursively step by step in order to obtain the optimal solution $\{\pi_t^*\}_{t=0}^{T-1}$, defined as $\pi_t^*(W_t, h_{t+1}) := arg\, max_{a\in\mathbb{A}}\, \mathbb{L}\phi_{t+1}(W_t, a, h_{t+1})$, and the value iteration

$$\begin{aligned}\phi_t\left(W_t, h_{t+1}\right) &= \mathbb{U}\phi_{t+1}\left(W_t, h_{t+1}\right) \\ &= \max_{a\in\mathbb{A}} \mathbb{E}_t\left[\phi_{t+1}\left(\mathbb{T}\left(W_t, a, h_{t+1}, Y_t\right)\right)\right], \quad t \in \{0,\ldots,T-1\}, \end{aligned} \tag{7}$$

with the obvious terminal condition $\phi_T(W_T) = U(\exp\{W_T\})$.

3. Solution to the Portfolio Optimization Problem

In this section, we present the solution to the portfolio optimization problem outlined in Section 2. Section 3.1 contains the main theoretical results. Section 3.2 elaborates on the theoretical foundations of evaluating suboptimal strategies and the comparison to the optimal solution via the wealth-equivalent loss.

3.1. Main Results

The optimal solution to Equation (5) is provided in the next theorem, which is followed by a corollary on the affine GARCH nature of the optimal wealth process.

Theorem 3.1 (Maximum expected utility representation): *Assume $\gamma < 0$, and let the log price of the risky asset follow an affine GARCH model, where for all $t \in \{0,\ldots,T-1\}$, and all admissible π_t and ν, the coefficients in* (2) *satisfy*

$$\frac{\partial^2}{\partial u^2} A(\gamma\pi_t, \nu; t, t+1) \geq 0 \quad \text{and} \quad \frac{\partial^2}{\partial u^2} B(\gamma\pi_t, \nu; t, t+1) \geq 0 \tag{8}$$

Then at time t, the maximum expected utility from terminal wealth can be written as

$$\phi_t\left(W_t, h_{t+1}\right) = \frac{1}{\gamma} \exp\left\{\gamma W_t + D_{t,T}\left(\pi_t^*\right) + E_{t,T}\left(\pi_t^*\right) \cdot h_{t+1}\right\}, \tag{9}$$

with $D_{t,T}$ and $E_{t,T}$ given by the recursive representations

$$D_{t,T}(\pi_t^*) = D_{t+1,T}(\pi_{t+1}^*) + \left(1-\pi_t^*\right)\gamma r + A\left(\gamma\pi_t^*, E_{t+1,T}(\pi_{t+1}^*); t, t+1\right), \tag{10a}$$

$$E_{t,T}(\pi_t^*) = B\left(\gamma\pi_t^*, E_{t+1,T}(\pi_{t+1}^*); t, t+1\right) + \frac{\gamma}{2}\left(\pi_t^* - \left(\pi_t^*\right)^2\right). \tag{10b}$$

with $E_{T,T} = D_{T,T} = 0$.

The optimal fraction of wealth invested in the risky asset at time t is given as a solution π_t^* *to the equations*

$$\frac{\partial}{\partial u} A(\gamma\pi_t, E_{t+1,T}(\pi_{t+1}^*); t, t+1) = r, \tag{11a}$$

$$\frac{\partial}{\partial u} B(\gamma\pi_t, E_{t+1,T}(\pi_{t+1}^*); t, t+1) = \pi_t - \frac{1}{2}. \tag{11b}$$

Moreover, a solution π_t^* *satisfying* (8), (11a), *and* (11b) *is a maximum.*

Note that an optimal solution is required to satisfy both equations in (11), which in general might not be possible. However, in the special cases of HN-GARCH (c.f. Heston and Nandi 2000) and IG-GARCH models (c.f. Christoffersen, Heston, and Jacobs 2006), (11a) is trivially satisfied and there remains only (11b) to solve.

Proof of Theorem 3.1: As outlined above, we use Bellman's value iteration in order to maximize via backwards induction and use the optimal solution at time $t+1$ for our approach at time t. In general, this results in the calculations below, where for the terminal step at time $t = T-1$ we just work with

$$\phi_T(W_T, h_{T+1}) := \phi_T(W_T) = U\left(\exp\{W_T\}\right) = \frac{1}{\gamma}\exp\{\gamma W_T\},$$

resulting in $D_{T,T} = E_{T,T} = 0$. We obtain:

$$\begin{aligned}
\phi_t(W_t, h_{t+1}) &= \max_{\pi_t} \mathbb{E}_t\left[\phi_{t+1}(W_{t+1}, h_{t+2})\right] \\
&= \max_{\pi_t} \mathbb{E}_t\left[\frac{1}{\gamma}\exp\left\{D_{t+1,T}(\pi_{t+1}^*) + \gamma W_{t+1} + E_{t+1,T}(\pi_{t+1}^*)\cdot h_{t+2}\right\}\right] \qquad (12) \\
&= \max_{\pi_t} \frac{1}{\gamma}\exp\left\{D_{t+1,T}(\pi_{t+1}^*)\right\} \\
&\quad \times \mathbb{E}_t\left[\exp\left\{\gamma\cdot\left[W_t + \pi_t(X_{t+1} - X_t) + \frac{1}{2}\left(\pi_t - \pi_t^2\right)h_{t+1}\right.\right.\right. \\
&\quad \left.\left.\left. + (1-\pi_t)r\right] + E_{t+1,T}(\pi_{t+1}^*)h_{t+2}\right\}\right] \\
&= \max_{\pi_t} \frac{1}{\gamma}\exp\left\{D_{t+1,T}(\pi_{t+1}^*) + (1-\pi_t)\gamma r + \gamma W_t + \frac{\gamma}{2}\left(\pi_t - \pi_t^2\right)h_{t+1}\right\} \\
&\quad \times \mathbb{E}_t\left[\exp\left\{\gamma\pi_t(X_{t+1} - X_t) + E_{t+1,T}(\pi_{t+1}^*)\cdot h_{t+2}\right\}\right] \\
&= \max_{\pi_t} \frac{1}{\gamma}\exp\left\{D_{t+1,T}(\pi_{t+1}^*) + (1-\pi_t)\gamma r + \gamma W_t + \frac{\gamma}{2}\left(\pi_t - \pi_t^2\right)h_{t+1}\right\} \\
&\quad \times \psi_{(X_{t+1}-X_t, h_{t+2})}\left(\gamma\pi_t, E_{t+1,T}(\pi_{t+1}^*)\middle|\mathcal{F}_t\right) \\
&= \max_{\pi_t} \frac{1}{\gamma}\exp\left\{D_{t,T}(\pi_t) + \gamma W_t + E_{t,T}(\pi_t)\cdot h_{t+1}\right\}, \qquad (13)
\end{aligned}$$

where we used the availability of the generating function in the affine GARCH setting according to (2) and define

$$D_{t,T}(\pi_t) = D_{t+1,T}(\pi^*_{t+1}) + (1-\pi_t)\,\gamma r + A\left(\gamma\pi_t, E_{t+1,T}(\pi^*_{t+1}); t, t+1\right) \tag{14a}$$

$$E_{t,T}(\pi_t) = B\left(\gamma\pi_t, E_{t+1,T}(\pi^*_{t+1}); t, t+1\right) + \frac{\gamma}{2}\left(\pi_t - \pi_t^2\right). \tag{14b}$$

Note that $\gamma < 0$ together with the second-order conditions in (8) are sufficient for the function in (13) to be concave in π_t. The first-order conditions in (11a) thus characterize the optimal solution to our portfolio problem. In particular, a solution satisfying (8), (11a), and (11b) is a maximum. ■

Corollary 3.2 (Affine GARCH process for optimal log wealth): *The optimal log wealth process $\{W_t\}_t$ follows an affine GARCH process. Furthermore, the optimal solution π_t^* does not depend on the conditional variance or the wealth.*

Proof: We start with the self-financing condition in Equation (4). The equation shows that the conditional variance of W_t is given by $\pi_{t-1}^2 h_t$. The affine GARCH representation for the optimal log wealth process can now be deduced from the proof of Theorem 3.1. That is, starting in line (12), disregarding the maximum operator and unnecessary factors, we can proceed to line (13) to solve the expectation below for the conditional bivariate moment generating function of W_t and h_{t+1}. Adopting also the definitions in (14a) results in:

$$\begin{aligned}\psi_{(W_t,h_{t+1})}(u,v|\mathcal{F}_{t-1}) &= \mathbb{E}_{t-1}\left[\exp\{uW_t + vh_{t+1}\}\right] \\ &= \exp\Big\{uW_{t-1} + (1-\pi_{t-1})\,ur + A\left(u\pi_{t-1}, v; t-1, t\right) \\ &\quad + \left(B\left(u\pi_{t-1}, v; t-1, t\right) + \frac{u}{2}\left(\pi_{t-1} - (\pi_{t-1})^2\right)\right)\cdot h_t\Big\}.\end{aligned}$$

This satisfies the requirements for affine GARCH processes outlined in Equations (1a) and (2). An investigation of the equations defining the optimal solution yields the second statement of our corollary. ■

It is not difficult to see that the HN-GARCH model (Heston and Nandi 2000), which has already been tackled in this context by Escobar-Anel, Gollart, and Zagst (2022), is a special case of Theorem 3.1. In particular, we introduce the set of parameters $\theta = (\lambda, \omega, \beta, \alpha, \rho)$ and an i.i.d. sequence $\{z_t\}_t$ of standard normal innovations. Then, choosing $f_1(h_t, \theta) = r + \lambda h_t$, $f_2(h_t, \theta) = \omega + \beta h_t$ and $f_3(h_t, z_t, \theta) = \alpha(z_t - \rho\sqrt{h_t})^2$, we obtain the following dynamics for the log return and its conditional variance process in the HN-GARCH model:

$$X_t - X_{t-1} = r + \lambda h_t + \sqrt{h_t} z_t, \tag{15a}$$

$$h_{t+1} = \omega + \beta h_t + \alpha\left(z_t - \rho\sqrt{h_t}\right)^2. \tag{15b}$$

3.2. Wealth-Equivalent Losses from Non-Optimal Strategies

In this subsection we establish a framework to evaluate suboptimal strategies and the loss that arises when following the associated wealth processes instead of the wealth from

our optimal solution. The utility derived from terminal wealth achieved via a suboptimal strategy $\{\pi_t^s\}_t$ is obtained via the tower property:

$$\begin{aligned}\phi_0^s(w_0,h_1) &= \mathbb{E}\left[U\left(V_T^s\right)\middle|\mathcal{F}_0\right] \\ &= \mathbb{E}\left[\mathbb{E}\left[\ldots\mathbb{E}\left[\mathbb{E}\left[U\left(V_T^s\right)\middle|\mathcal{F}_{T-1}\right]\middle|\mathcal{F}_{T-2}\right]\cdots\middle|\mathcal{F}_1\right]\middle|\mathcal{F}_0\right],\end{aligned} \tag{16}$$

where V_T^s is the final wealth corresponding to strategy $\{\pi_t^s\}_t$ and $w_0 = \log v_0$. For the sake of comparability, we assume the same transition law for suboptimal strategies as for the optimal solution, i.e., we work with the proxy W_t of the log wealth process $\log V_t$, derived via the approximation of the self-financing condition (see Equations (4) and (6)). We refer to Section 5.1 for an investigation concerning the impact of using this approach. This yields the following equation for the expected utility from terminal wealth at time $t \in \{0,\ldots,T-1\}$:

$$\phi_t^s(W_t,h_{t+1}) = \mathbb{E}\left[\phi_{t+1}^s\left(\mathbb{T}\left(W_t,\pi_t^s,h_{t+1},Y_{t+1}\right)\right)\middle|\mathcal{F}_t\right], \tag{17}$$

with $Y_{t+1} = X_{t+1} - X_t$ and the terminal condition $\phi_T^s(W_T) = U(\exp\{W_T\})$. Referring to Escobar, Ferrando, and Rubtsov (2015), we define the wealth-equivalent loss from following the suboptimal strategy $\{\pi_t^s\}_t$ instead of $\{\pi_t^*\}_t$ as the solution L_t^s to

$$\phi_t\left(\log\left(V_t\cdot\left(1-L_t^s\right)\right),h_{t+1}\right) = \phi_t^s\left(\log\left(V_t\right),h_{t+1}\right). \tag{18}$$

This suggests the interpretation that an investor following the optimal investment strategy needs a fraction of L_0^s less initial wealth to achieve the same expected utility as another investor using the suboptimal portfolio process $\{\pi_t^s\}_t$. From Equations (9) and (18), we directly deduce that

$$L_t^s = 1 - \exp\left\{\frac{1}{\gamma}\cdot\left(D_{t,T}^s - D_{t,T}^*\right) + \left(E_{t,T}^s - E_{t,T}^*\right)\cdot\frac{h_{t+1}}{\gamma}\right\}, \tag{19}$$

with $D_{t,T}^* = D_{t+1,T}(\pi_{t+1}^*)$, $E_{t,T}^* = E_{t+1,T}(\pi_{t+1}^*)$, and the following recursive law for $D_{t,T}^s$ and $E_{t,T}^s$:

$$D_{t,T}^s\left(\pi_{t+1}^s\right) = D_{t+1,T}^s\left(\pi_{t+1}^s\right) + \left(1-\pi_t^s\right)\gamma r + A\left(\gamma\pi_t^s, E_{t+1,T}^s\left(\pi_{t+1}^s\right); t, t+1\right), \tag{20a}$$

$$E_{t,T}^s\left(\pi_{t+1}^s\right) = B\left(\gamma\pi_t^s, E_{t+1,T}^s\left(\pi_{t+1}^s\right); t, t+1\right) + \frac{\gamma}{2}\left(\pi_t^s - \left(\pi_t^s\right)^2\right), \tag{20b}$$

with the usual terminal conditions $D_{T,T}^s = E_{T,T}^s = 0$.

4. Application to IG-GARCH Model

In this section, we present the inverse Gaussian GARCH (IG-GARCH) model (c.f. Christoffersen, Heston, and Jacobs 2006) as a special case of our main result. Assume the following dynamics for the log return $X_t - X_{t-1} = \log S_t - \log S_{t-1}$ and its conditional

variance process $h = \{h_t\}_{t=1,\dots,T}$:

$$X_t - X_{t-1} = r + \nu h_t + \eta y_t, \tag{21a}$$

$$h_{t+1} = w + b h_t + c y_t + a \frac{h_t^2}{y_t}, \tag{21b}$$

with $\eta < 0$ and $\{y_t\}_t$ a sequence of random variables with inverse Gaussian distribution and single parameter $\delta_t = \delta(t) = h_t/\eta^2$. In particular, translating this single-parameter form to the known representation of an inverse Gaussian distribution, we have $y_t \sim IG(\delta_t, \delta_t^2)$ and $\mathbb{E}_{t-1}[y_t] = Var_{t-1}[y_t] = \delta_t$.

Comparing Equations (21a) to (1a), we first note that scaling of the inverse Gaussian random variable with some parameter α yields $\alpha y_t \sim IG(\alpha\delta_t, \alpha\delta_t^2)$. This implies that, in order to obtain the form of (1a), we need to define $\xi_t \sim IG(-\sqrt{\delta_t}, \sqrt{\delta_t}^3) = IG(-\sqrt{h_t}/\eta, \sqrt{h_t}^3/\eta^3)$, where, from the variance of a two-parameter inverse Gaussian variable, we obtain $Var_{t-1}[\xi_t] = 1$. The minus for the first parameter compensates for $\eta < 0$ to meet the requirement of positive parameters in the IG distribution. Standardizing this random variable further w.r.t. the mean by subtracting $-\sqrt{h_t}/\eta$ finally allows us to present the embedding of the IG-GARCH model into the general setting by Badescu, Cui, and Ortega (2019). With a set of parameters denoted by $\theta = (\nu, \eta, w, b, c, a)$, we have

$$f_1(h_t, \theta) = r + \nu \cdot h_t, \quad f_2(h_t, \theta) = w + b \cdot h_t, \quad f_3\left(h_t, y_t, \theta\right) = c y_t + a \frac{h_t^2}{y_t},$$

where $\{\epsilon_t\}_t$, $\epsilon_t = \xi_t + \sqrt{h_t}/\eta$, are standardized inverse Gaussian random variables. However, we usually work with $\tilde{f}_1 = r + (\nu + \frac{1}{\eta})h_t$ and use $\{\xi_t\}_t$ as innovations in (1a). From this mean-standardized formulation, we derive the market price of risk as $\lambda = \nu + \frac{1}{\eta}$.[1]

Remark 4.1 (Inverse Gaussian innovations): (i) Note that the shape of y_t still depends on h_t, thus the IG-GARCH model only fulfils a relaxation of the condition on the sequence of shocks in the general affine setting. In particular, instead of explicitly relying on the innovations $\{\epsilon_t\}_{t=1,\dots T}$ (or $\{\xi_t\}_{t=1,\dots T}$) in (1a) being i.i.d., we require that the choice of distribution allows for the exponentially affine representation of the conditional bivariate generating function in (2). This slight adjustment accommodates the IG-GARCH model while preserving the necessary and important properties of our framework.

(ii) Via sending $\eta \to 0$, the skewness $\mathcal{S}$ and excess kurtosis $\mathcal{K}$ on the one-step distribution, which are determined by (c.f. Christoffersen, Heston, and Jacobs 2006)

$$\mathcal{S}_t[X_{t+1} - X_t] = 3\eta (h_{t+1})^{-1/2}, \quad \mathcal{K}_t[X_{t+1} - X_t] = 15\eta^2 (h_{t+1})^{-1}, \tag{22}$$

vanish and the standardized shock becomes standard normal in the limit. This can be used to derive the continuous-time Heston model (Heston 1993) in the limit (cf. Christoffersen, Heston, and Jacobs 2006, p. 258).[2]

The first two conditional moments of the log return are provided next, where we use the length of a time step being exactly one day, i.e., $\Delta = 1$.

$$\mathbb{E}_t\left[X_{t+1} - X_t\right] = r + \left(\nu + \frac{1}{\eta}\right) \cdot h_{t+1}, \tag{23}$$

$$Var_t\left[X_{t+1}\right] = h_{t+1}. \tag{24}$$

The following corollary applies our main results to the IG-GARCH setting.

Corollary 4.2 (IG-GARCH model): *Assuming existence, the optimal solution to the stochastic control problem in* (5)*, with the log price dynamics represented in the form of* (21)*, is given as a real solution to the equation*

$$\nu + \frac{\sqrt{\left(1 - 2E^*_{t+1,T} a\eta^4\right)}}{\eta\sqrt{\left(1 - 2\eta\gamma\pi_t - 2E^*_{t+1,T} c\right)}} = \pi_t - \frac{1}{2}, \tag{25}$$

if the following two conditions are satisfied for all admissible values of π_t *and all* $t \in \{0, \ldots, T-1\}$ *:*

$$1 - 2E^*_{t+1,T} a\eta^4 \geq 0 \quad \text{and} \quad 1 - 2\eta\gamma\pi_t - 2E^*_{t+1,T} c > 0. \tag{26}$$

The solutions of Equation (25) *can be found via the roots of a cubic polynomial with real coefficients, and there is exactly one real solution if the discriminant of this polynomial is negative. A solution* π_t^* *satisfying* (25) *and* (26) *is a maximum.*

Proof: As of Christoffersen, Heston, and Jacobs (2006), the coefficients A and B of the conditional bivariate moment generating function in (2) in the IG-GARCH model are given by

$$\begin{aligned} A\left(\gamma\pi_t, E^*_{t+1,T}; t, t+1\right) &= r\gamma\pi_t + E^*_{t+1,T} w - \frac{1}{2}\log\left(1 - 2E^*_{t+1,T} a\eta^4\right), \\ B\left(\gamma\pi_t, E^*_{t+1,T}; t, t+1\right) &= E^*_{t+1,T} b + \nu\gamma\pi_t + \eta^{-2} \\ &\quad - \eta^{-2}\sqrt{\left(1 - 2E^*_{t+1,T} a\eta^4\right)\left(1 - 2\eta\gamma\pi_t - 2E^*_{t+1,T} c\right)}, \end{aligned}$$

with $E^*_{t+1,T} := E_{t+1,T}(\pi^*_{t+1})$. Combining these formulas with Theorem 3.1, we obtain the explicit representations for $D_{t,T}$ and $E_{t,T}$ in terms of the parameters of the IG-GARCH model:

$$D_{t,T} = D_{t+1,T} + \gamma r + E^*_{t+1,T} w - \frac{1}{2}\log\left(1 - 2E^*_{t+1,T} a\eta^4\right), \tag{27a}$$

$$\begin{aligned} E_{t,T}\left(\pi_t\right) &= \frac{\gamma}{2}\left(\pi_t - \pi_t^2\right) + E^*_{t+1,T} b + \nu\gamma\pi_t \\ &\quad + \eta^{-2}\left(1 - \sqrt{\left(1 - 2E^*_{t+1,T} a\eta^4\right)\left(1 - 2\eta\gamma\pi_t - 2E^*_{t+1,T} c\right)}\right). \end{aligned} \tag{27b}$$

Thus, the two Equations (11a) and (11b) reduce to (25), which needs to be solved for π_t in order to obtain the optimal fraction invested in the risky asset. With the second-order conditions (26) fulfilled, we deduce that a solution must be a maximum.

Working towards solving Equation (25), we first isolate the radicals, square the equation and rearrange terms in order to obtain the following cubic equation:

$$\begin{aligned}
&\frac{1-2E^*_{t+1,T}a\eta^4}{\eta^2\cdot\left(1-2\eta\gamma\pi_t-2E^*_{t+1,T}c\right)}\\
&\quad=\pi_t^2-(1+2\nu)\cdot\pi_t+\left(\nu+\frac{1}{2}\right)^2\\
&\quad\Leftrightarrow\frac{1}{\eta^2}\cdot\left(1-2E^*_{t+1,T}a\eta^4\right)=-2\eta\gamma\pi_t^3+\left(1-2E^*_{t+1,T}c\right)\pi_t^2\\
&\qquad+2\eta\gamma\,(1+2\nu)\cdot\pi_t^2-(1+2\nu)\left(1-2E^*_{t+1,T}c\right)\pi_t\\
&\qquad-2\eta\gamma\left(\nu+\frac{1}{2}\right)^2\pi_t+\left(1-2E^*_{t+1,T}c\right)\left(\nu+\frac{1}{2}\right)^2\\
&\quad\Leftrightarrow p_3\cdot\pi_t^3+p_2\cdot\pi_t^2+p_1\cdot\pi_t+p_0=0,
\end{aligned}\tag{28}$$

where the coefficients of the polynomial in (28) are given by

$$p_3=2\eta\gamma,\tag{29a}$$

$$p_2=-2\eta\gamma\,(2\nu+1)-\left(1-2E^*_{t+1,T}c\right),\tag{29b}$$

$$p_1=2\eta\gamma\left(\nu+\frac{1}{2}\right)^2+(2\nu+1)\cdot\left(1-2E^*_{t+1,T}c\right),\tag{29c}$$

$$p_0=\frac{1}{\eta^2}\left(1-2E^*_{t+1,T}a\eta^4\right)-\left(\nu+\frac{1}{2}\right)^2\cdot\left(1-2E^*_{t+1,T}c\right).\tag{29d}$$

The polynomial in (28) has three roots, and the number of real solutions among these can be deduced from the sign of the discriminant of the polynomial, which in the cubic case is known to be

$$\mathcal{D}=18p_3p_2p_1p_0+p_2^2p_1^2-4p_3p_1^3-4p_2^3p_0-27p_3^2p_0^2.$$ ■

The fact that the number of real solutions of a cubic polynomial can be deduced from the sign of its discriminant makes it worth pointing out that in Equation (29a), the arrangement ensures that the signs of three coefficients can easily be derived. Here, we take into account Condition (26) and use that both η and γ are assumed to be strictly negative, while – according to the estimates by Christoffersen, Heston, and Jacobs (2006, Table 2) and, more recently, by Babaoğlu et al. (2018, Table 2) – ν is positive with order of magnitude 3. In particular, we have $p_3>0$ and $p_1>0$, while $p_2<0$ and no immediate decision can be made for p_0. However, from this position, the sign of $\mathcal{D}$ cannot be told immediately. We thus refer to our numerical analyses in Section 5.1, which show that for relevant values of γ, we have exactly one real solution to the optimality equation.

Note that we can make sure that Condition (8) is satisfied by assuming that the arguments of both square roots in (25) are positive, i.e., both inequalities in (26) are fulfilled with strict inequality. In fact, this implicitly imposes conditions on π_t^*, which need to be checked in practice. However, due to the order of magnitude of the parameter η being 10^{-4}

Table 1. Values for the parameters used in the IG-GARCH portfolio optimization problem – consisting of the ML estimates for all IG-GARCH parameters as of Christoffersen, Heston, and Jacobs (2006), called *IG Set 1*, and Babaoğlu et al. (2018), called *IG Set 2*, respectively, and of the default choices for the investment parameters.

Panel A: IG-GARCH Parameters			Panel B: Inv. Params.	
Parameter	IG Set 1	IG Set 2	Parameter	Def. Val.
ν	1.625e3	1.747e3	T	252
η	−6.162e−4	−5.729e−04	r	0.01/252
w	3.768e−10	−1.469E−06	v_0	1.00
a	2.472e7	3.190e+7	γ	−1
b	−1.933e1	−2.182e1		
c	4.142e−6	4.047e−6		

(considering the estimates from Christoffersen, Heston, and Jacobs (2006) and Babaoğlu et al. (2018) again), the conditions can be expected to be satisfied at least by the optimal terminal solution.

5. Numerical Analysis

This section is divided in three parts: Section 5.1 studies the number of real solutions of the optimality Equation (25) and the quality of the second-order approximation of the SFC (4). Section 5.2 evaluates the sensitivity of the optimal solution to the different parameters of our model, referring to IG-GARCH as well as investment parameters. We also compare our solution to the embedded case of an HN-GARCH model (presented in Escobar-Anel, Gollart, and Zagst 2022) and show the impact of skewness and kurtosis on allocation and value function. The last part in this section studies wealth-equivalent losses when the decision maker uses sub-optimal strategies, in particular when using the HN-GARCH framework or Merton's solution instead of the IG-GARCH strategy presented in this paper.

The analyses in this section will be based on two different sets of maximum likelihood estimates for the IG-GARCH model, taken from Christoffersen, Heston, and Jacobs (2006, Table 2) and Babaoğlu et al. (2018, Table 2), which are presented together in Table 1, Panel A. The former set of MLEs for the IG-GARCH parameters will be called *IG Set 1*, the latter one *IG Set 2*. If not stated otherwise, a one-year time horizon (i.e., $T = 252$ days) is assumed, the risk-free rate is set to $r = 0.01/252$, the initial amount of wealth is $v_0 = 1$, while the risk aversion parameter is set at $\gamma = -1$. A summary of the investment parameters can also be found in Panel B of Table 1.

5.1. Feasibility of Solution and Approximation

The number of real solutions to the optimality Equation (25) can be deduced from the sign of the discriminant of the cubic polynomial in (28) with the coefficients from (29a). Figure 1 takes the ML estimates from IG Set 1 and shows that, since we assume $\gamma < 0$, the discriminant is negative for all relevant values of γ. The first plot evaluates the discriminant for $\gamma \in [-5, 1)$. In contrast to the purple dots, the red ones show that the value is non-negative, which clearly is only the case for some γ-values strictly greater than zero. The shape of the discriminant in the critical range can be observed from the second plot. We note that when replacing the ML estimates from IG Set 1 by IG Set 2, this does not

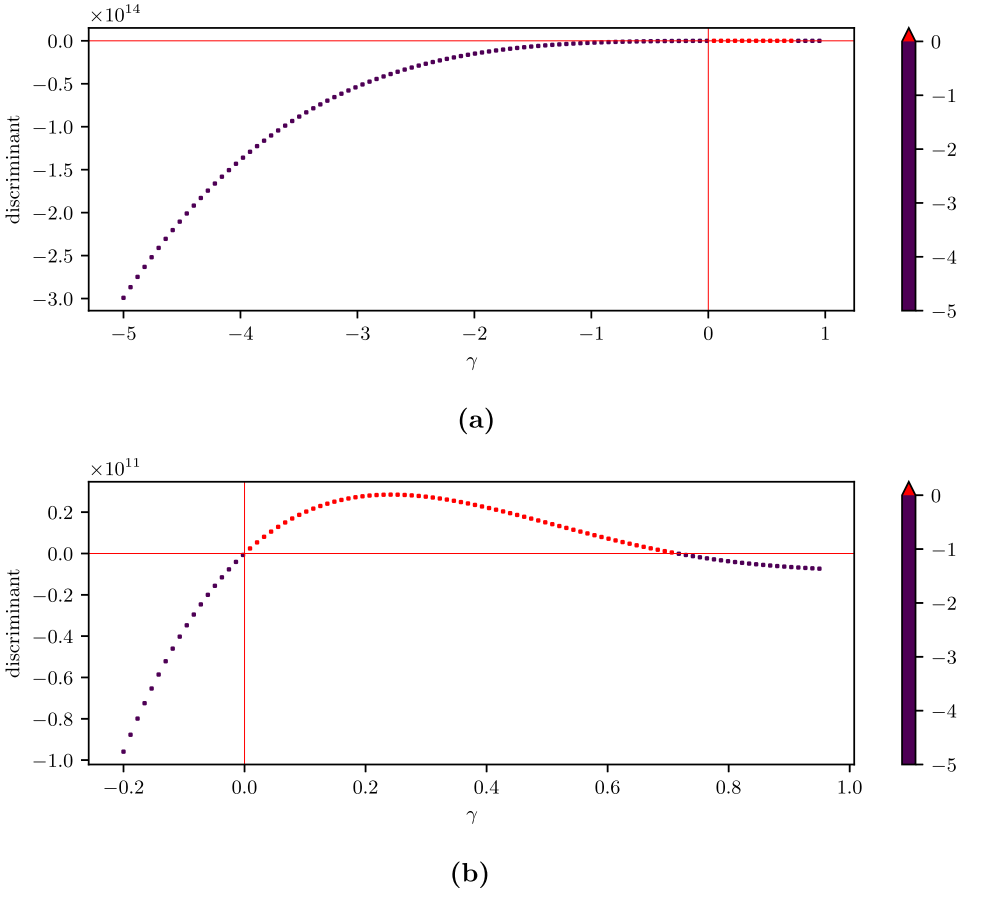

Figure 1. Discriminant of optimality polynomial, dependent on γ. Parameter estimates from IG Set 1. The two plots show that the value of the discriminant is negative for the relevant area of γ below zero. (a) Discriminant values for $\gamma \in [-5, 1)$. (b) Discriminant values for $\gamma \in [-0.2, 1)$.

significantly change the picture. Therefore, for the parameter settings relevant to us, we obtain exactly one real solution from solving the optimality Equation (25), which henceforth will be called *the optimal solution*. Furthermore, note that the unique real solution is a maximum, since the conditions stated in Corollary 4.2 are satisfied. In particular, while Equation (25) represents the first-order condition, the choice $\gamma < 0$ together with the two inequalities in (26) (evaluated at π_t^*) ensure that the second derivative of the objective function (13) with respect to π_t is negative at the optimum.

As stated in Section 2, we use an approximation of the self-financing condition in our model, which is developed via a second-order Taylor expansion. The wealth process, with the exact self-financing condition, actually evolves according to Formula (3). In our model, we work with e^{W_t}, W_t being the approximation of the log wealth (see (4)). V_t and e^{W_t} are equal at any initial time, e.g., $w_0 = \log v_0$, but they grow apart as time evolves.

To assess the difference between the two processes $\{V_t\}_t$ and $\{e^{W_t}\}_t$, we perform two analyses assuming IG Set 1 (see Table 1) with $T = 5 \cdot 252$. For the first analysis, we simulate 100,000 paths over a trading period of five years and compute the distributions of V_T and

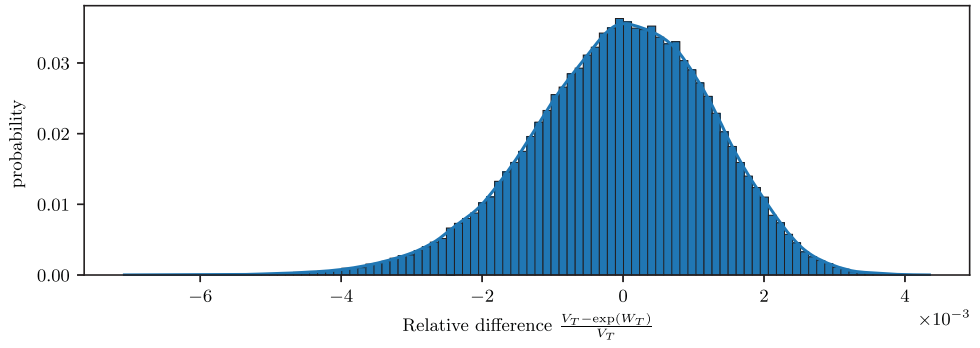

Figure 2. Comparison of the two wealth processes at time $T = 5 \cdot 252$, with IG Set 1. The curve is bell-shaped and the vast majority of values is between -0.4% and $+0.4\%$ of the initial wealth.

e^{W_T}. Figure 2 shows the difference between the terminal values of both processes relative to the level of wealth. The difference appears to be centred around zero with the vast majority of values gathered between -0.4% and $+0.4\%$ of the initial wealth at time $t = 0$.[3]

For the second analysis in this regard, we take into account the fact that our optimal wealth process is not self-financing. This implies that a decision maker following the suggested strategy needs to pay in or withdraw money in each iteration in order to set her actual wealth V_t equal to e^{W_t}. The distribution of the amount of money necessary for the adjustment, again obtained from 100,000 simulations over a time period of five years, is shown in Figure 3. In the first plot, Figure 3(a), we observe that the distribution of the adjustment values is right-skewed. This means that the decision maker is more likely to withdraw small amounts of money for the adjustment, but in case of paying in, the amount might be larger.[4] The distribution of the accumulated amount of money to be added to or withdrawn from the portfolio strategy, displayed in Figure 3(b), is centred around zero, with 97.08% of values in the interval $[-0.5\%, 0.5\%]$ of the initial wealth. The analysis furthermore shows that putting an additional amount of 1% of the initial wealth aside at the beginning suffices in almost a hundred percent of all cases in order to manage all adjustments over a five-years investment horizon. The corresponding analysis using the second set of parameter estimates produces even better results, see Appendix A.1.1.

5.2. Parameter Sensitivity

This subsection explores the sensitivity of the optimal strategy to the IG-GARCH and investment parameters. Our investigation consists of three main parts: We first study the dependence of the optimal solution on the time horizon T, and on the decision maker's level of risk aversion, which is determined by γ. Then, we focus on the key parameter creating the one-period non-Gaussian distribution: η. This parameter controls the skewness and kurtosis of the asset returns, separating the IG-GARCH from the HN-GARCH. Studies concerning the remaining IG-GARCH parameters follow.

Regarding the time horizon T, since π_0^* is calculated via backwards iteration from π_{T-1}^*, the optimal initial solution directly depends on the planning horizon. Figure 4 shows the value of the optimal initial solution to our portfolio problem (using both introduced sets of parameter estimates, see Table 1) for a time horizon ranging from one day to five years,

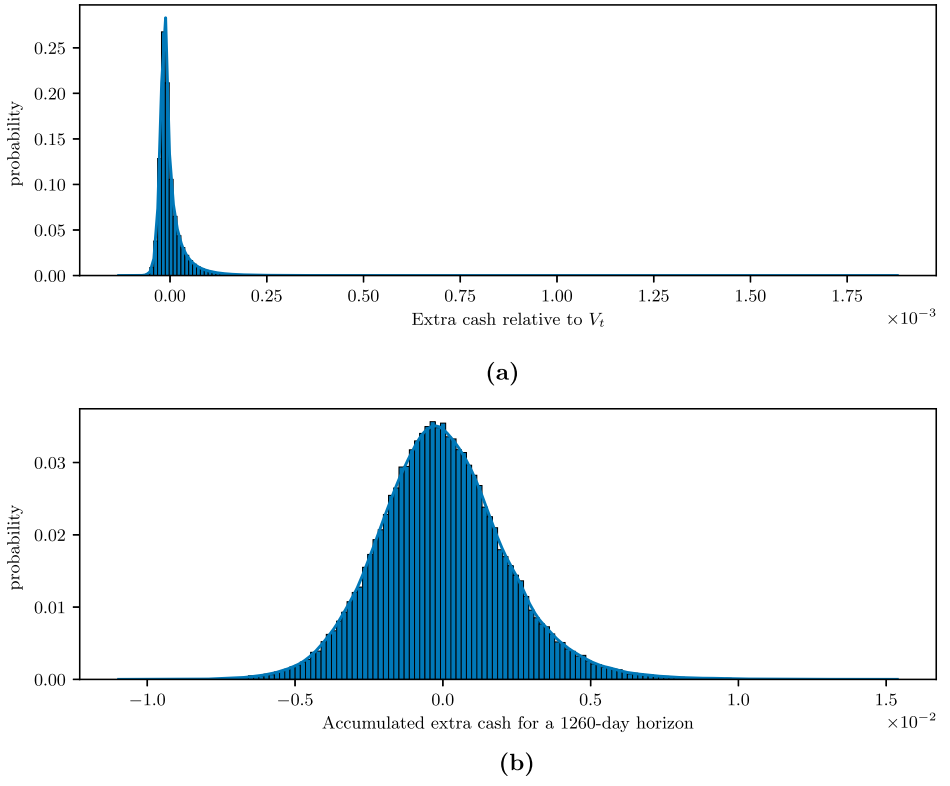

Figure 3. Extra cash needed for setting $V_t = e^{W_t}$ in each iteration, using IG Set 1. The plots indicate that the accumulated amount of extra cash is very likely to be between −1% and +1%. In 97.08% of all cases, the absolute value is below 0.5%. (a) Histogram of adjustments in all simulations, over the whole time horizon. (b) Histogram of the accumulated amount of extra cash needed over the whole time horizon.

assuming 252 trading days per year. The two plots show similar behaviour of the solution, both increasing in a short-range with a steep convergence, e.g., sensitive to changes of the time horizon only for T less than one year.

On the other hand, the plots in Figure 5 show that π_0^* has a significant dependence on the investor's level of risk aversion. The figure confirms that as we decrease γ, the level of risk aversion increases, which is consistent with the decrease in the share of wealth invested in the risky asset observed in both plots in Figure 5.

We turn our attention to η as the key source of non-Gaussianity and its impact on portfolio decisions. In order to isolate the non-Gaussian behaviour, we study the impact of changes in η while keeping the expected return and the variance unchanged, i.e., the unconditional first and second-order moments. Thus, when changing η, we also adapt the remaining parameters of the IG-GARCH model. These additional adjustments can be expressed most easily using the parameters $(\lambda, \omega, \beta, \alpha, \rho)$ of an artificial HN-GARCH model[5], which exactly matches the first two moments of the prevailing IG-GARCH. This possible calibration of the two models was already noted in Christoffersen, Heston, and Jacobs (2006). In particular, for any η, we modify ν according to $\nu(\eta) = \lambda - \eta^{-1}$, while $w(\eta) = \omega$ and (a, b, c) are adapted as follows:

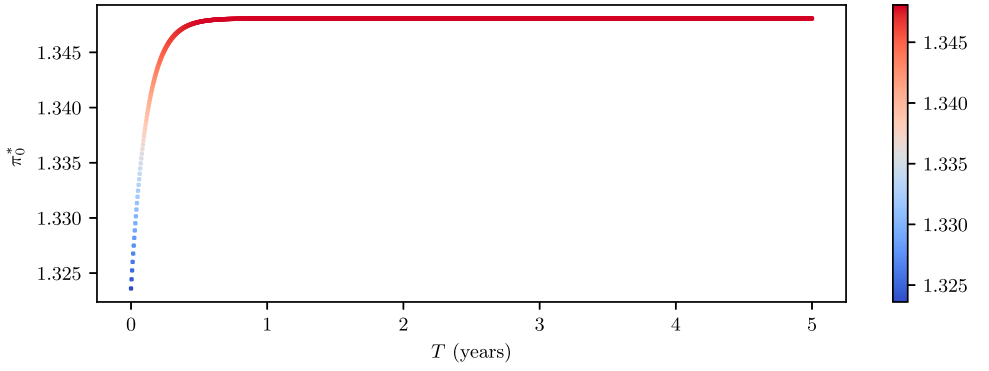

(a)

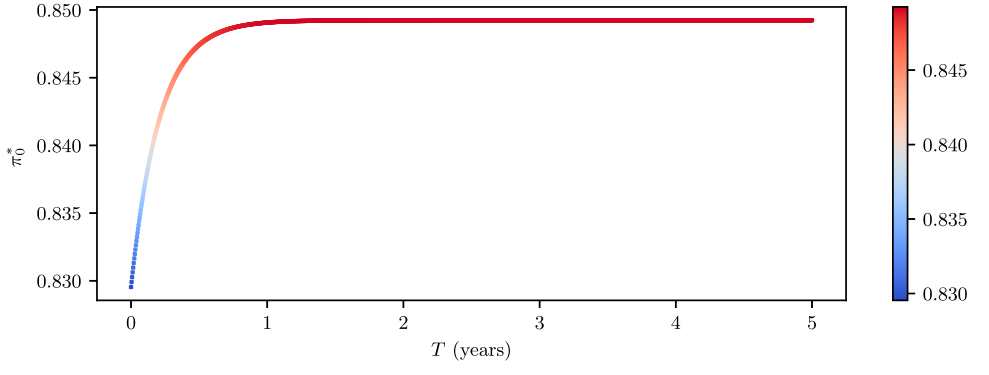

(b)

Figure 4. Dependence of the initial solution π_0^* on the planning horizon T, displayed in years. The two curves evolve nearly identical, showing a steep increase of around two percentage points in less than one year and remaining stable at this level henceforth. (a) IG Set 1. (b) IG Set 2.

$$a(\eta) = \frac{\alpha}{\eta^4}, \quad b(\eta) = \beta + \alpha\rho^2 - \frac{2\alpha}{\eta^2} + \frac{2\alpha\rho}{\eta}, \quad c(\eta) = \alpha - 2\eta\alpha\rho.$$

As a result, any IG-GARCH parametrization $(\eta, \nu(\eta), w(\eta), a(\eta), b(\eta), c(\eta))$ calibrated with the same set $(\lambda, \omega, \beta, \alpha, \rho)$ of HN-GARCH parameters yields the same first and second moments.

In this context, the plots in Figure 6 exhibit decreasing fractions of wealth invested in the risky asset with decreasing skewness and increasing (excess) kurtosis. This finding is compatible with the intuition that an increase of excess kurtosis (more extreme events) combined with negative skewness (negative events) means a higher probability of losses, hence a reduction of risky investment. Note, however, that the plotted range for η yields very extreme values for skewness and excess kurtosis at its lower end and is chosen for illustrative purposes. Figure 6(a) shows how the optimal initial solution depends on η for different levels of risk aversion, expressed via the parameter γ. The plot in Figure 6(b) isolates the dependency of the optimal solution on skewness and kurtosis, here we fix $\gamma =$

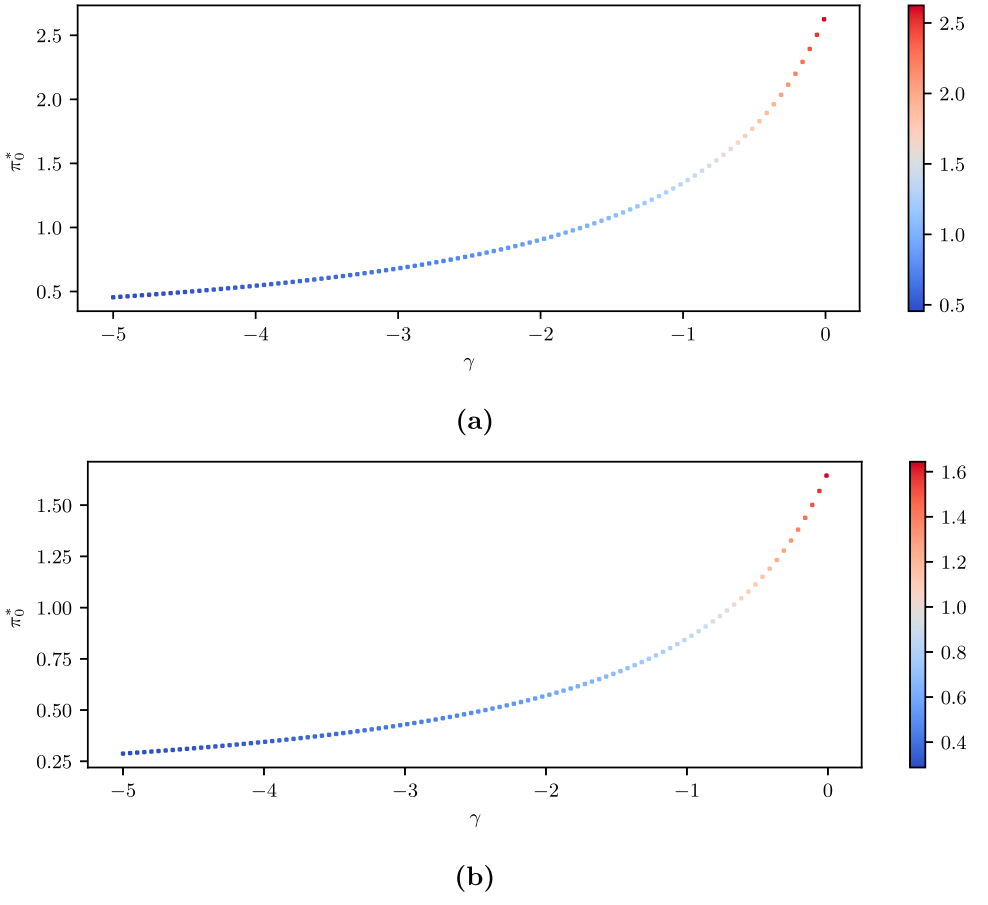

Figure 5. Dependence of the initial solution on the level of risk aversion in the different parameter settings (see Table 1) with a one-year time horizon ($T = 252$). The range for γ is $[-5, -0.01]$. In both cases, the fraction of wealth increases with γ. (a) IG Set 1. (b) IG Set 2.

-1. The IG-GARCH solution changes with respect to the parameter η, again showing a less risky allocation as η decreases.

We now proceed to study the impact on the optimal allocation of the remaining parameters in the model, which are (a, b, c, ν)[6]. The impact of ν on our optimal solution is investigated directly via the market price of risk $\lambda = \nu + \eta^{-1}$. For our analysis, we keep η constant and move ν to evaluate the sensitivity. Figure 7 clearly shows that as the market price of risk increases, the fraction of wealth invested in the risky asset also increases significantly. The plot displays this analysis for IG Set 1, switching to the estimates in IG Set 2 yields identical results on a generally lower level in terms of π_t^*. The corresponding Figure can be found in Appendix A.1.2.

We plot the impact of (a, b, c) in Figure 8. Recalling that the unconditional variance of the log return in the IG-GARCH model is given by $(w + a\eta^4)/(1 - a\eta^2 - b - c/\eta^2)$, we first note that in order to keep this term positive, neither a nor b and c can be increased much without further adjustments. Since numerical examinations show that the above mentioned condition is violated even for very little increases, we restrict our analysis to

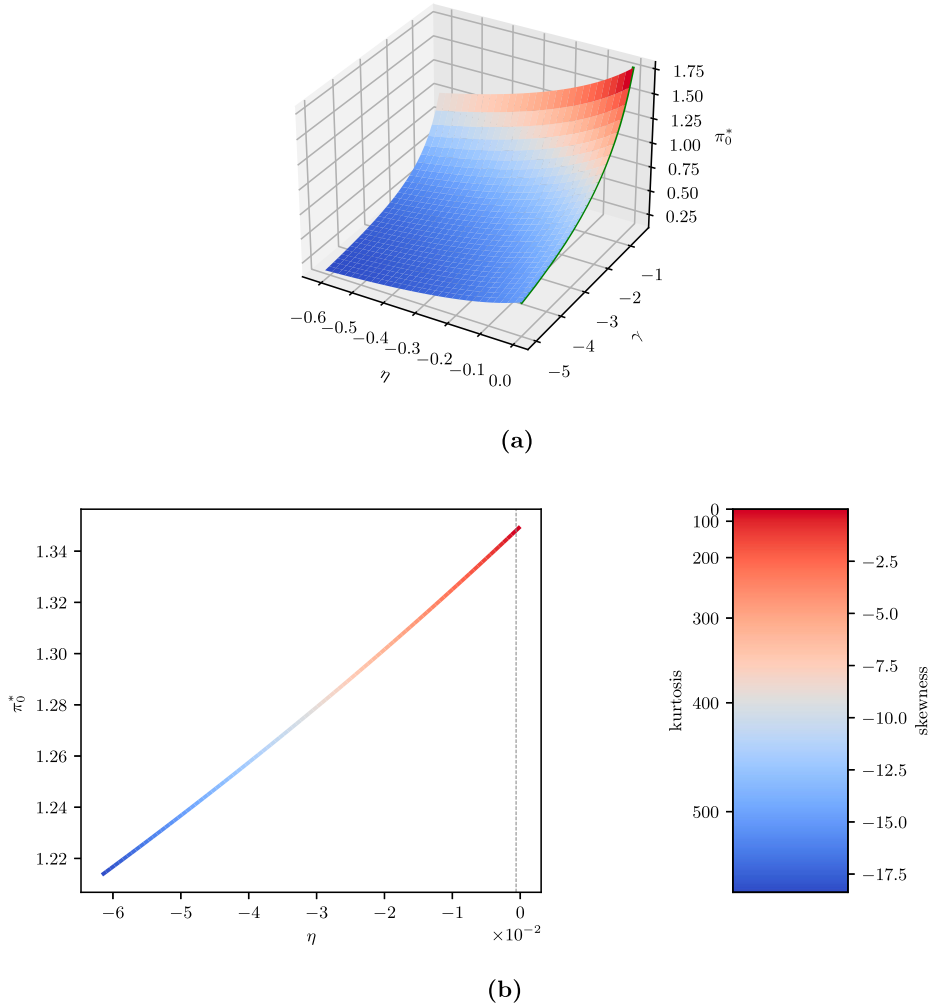

Figure 6. Dependence of π_0^* on γ and η (Part 6(a)) and on η alone (Part 6(b)) for a one-year time horizon. The prevailing IG-GARCH parameter estimates are from IG Set 1 (see Table 1), the analysis for the alternative parameter setting can be found in Appendix A.1.2. (a) π_0^* dependent on γ and η. The x-axis scales the original estimate for η by a factor of at most 1×10^3, the range for γ is $[-5, -0.5]$. (b) π_0^* dependent on η only, with $\gamma = -1$. Here, η is scaled by at most 1×10^2. The colour bar indicates the corresponding values of skewness and kurtosis of the distribution of log asset return innovations.

decreases in these parameters. In all cases, decreasing the parameter value decreases the fraction of wealth invested in the risky asset. Note the limit of π_0^* when decreasing a, b, or c corresponds with the value of the terminal solution π_{T-1}^*, which can be observed also in the plot for the alternative parameter setting, shown in Appendix A.1.2. Hence, decreasing these parameters seems to flatten the curve in Figure 4.

5.3. Wealth-equivalent Losses and Comparison to HN-GARCH

In this last part of the numerical analysis, we start by comparing the optimal strategies of the two GARCH models, i.e., IG-GARCH and HN-GARCH (as of Escobar-Anel, Gollart,

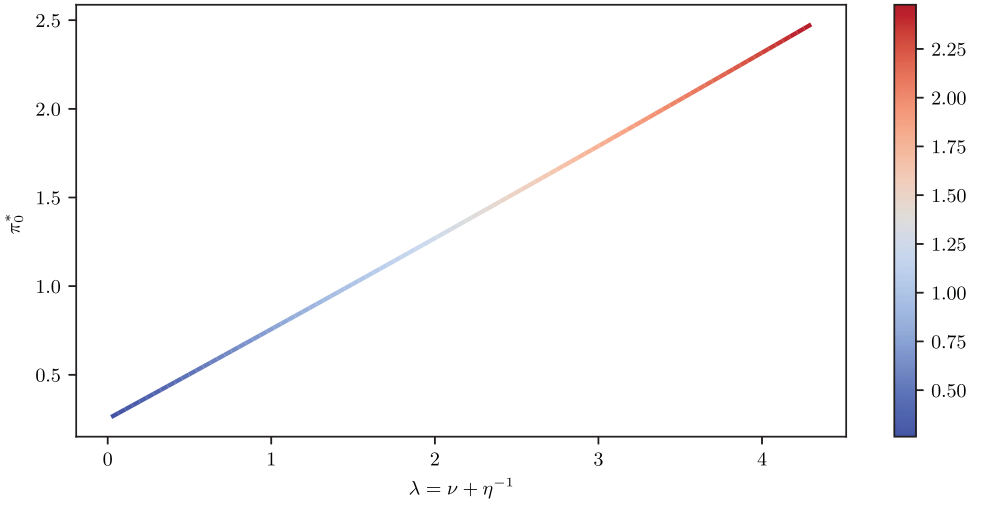

Figure 7. Dependence of π_0^* on the market price of risk for a one-year time horizon, using IG Set 1. The optimal initial solution increases significantly with λ.

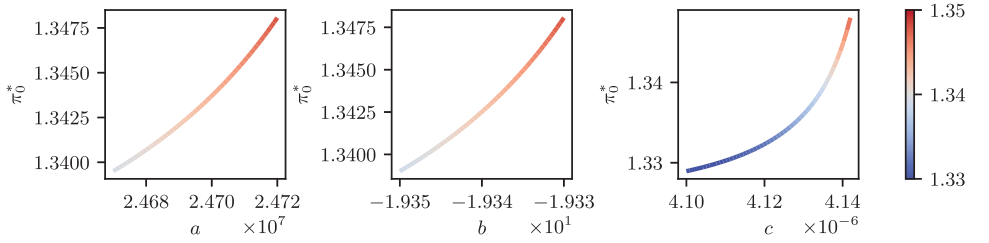

Figure 8. Dependence of π_0^* on a, b and c, respectively. The time horizon is $T = 252$, we use IG Set 1. For all three plots, decreasing the parameter from its original estimate decreases the initial solution gradually towards the level of the terminal solution.

and Zagst 2022). Subsequently, we evaluate the performance of our solution against two different benchmarks, first the solution of the Gaussian HN-GARCH model, and second Merton's popular static solution (c.f. Merton 1969). Concerning the parameters of the IG-GARCH model, we base our analyses on the two sets in Table 1. For the HN-GARCH model (15a), we use analogous maximum likelihood estimates from the same sources (Christoffersen, Heston, and Jacobs 2006; Babaoğlu et al. 2018), presented together in Table 2. The latter two sets of estimates will be called *HN Set 1* and *HN Set 2*, respectively. In particular, IG Set 1 and HN Set 1 are obtained via fitting the corresponding model to the same data set.[7] That is, our analysis is based on the assumption that the investor observes the market data and derives the MLEs for the model parameters for IG-GARCH, HN-GARCH or a homoskedastic Gaussian model, where the latter forms the base for calculating Merton's static solution (Merton 1969). Based on these parameters, the optimal solution in the three models are determined, and their performance is compared under the premise that 'real' log asset returns follow an IG-GARCH model.

Table 2. Maximum likelihood estimates for the parameters of the HN-GARCH model, as of Christoffersen, Heston, and Jacobs (2006) (*HN Set 1*) and Babaoğlu et al. (2018) (*HN Set 2*), respectively.

Parameter	HN Set 1	HN Set 2
λ	2.772e 0	1.10e0
ω	3.038e−09	−1.396e−6
β	9.026e−01	9.00e−1
α	3.660e−06	3.761e−6
ρ	1.284e+2	1.457e2

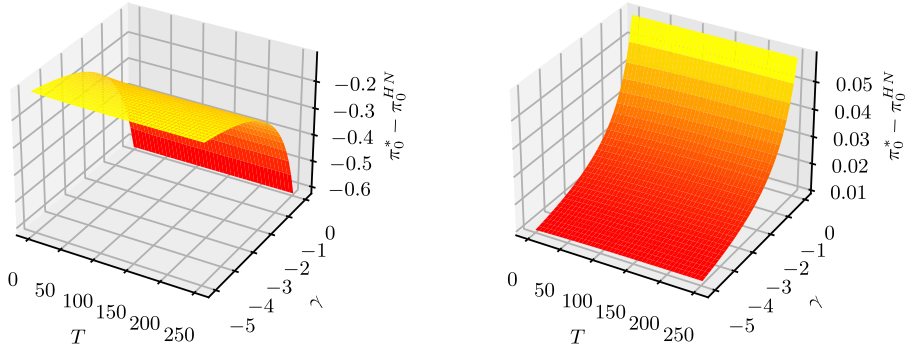

Figure 9. Comparison of the optimal solutions in the IG-GARCH and the HN-GARCH framework over a time horizon of one year, dependent on the level of risk aversion, represented via the parameter $\gamma \in [-5, -0.01]$. In both cases, the difference increases with γ. For Set 1, the HN-GARCH yields a larger value for the optimal solution, while for Set 2, this relation is reversed. The difference does not change significantly with the time horizon T. (a) Set 1. (b) Set 2.

Figure 9 shows a comparison of optimal allocation in both GARCH models, i.e., IG and HN, using the corresponding IG and HN estimates from Sets 1 and 2. Note that Christoffersen, Heston, and Jacobs (2006) and Babaoğlu et al. (2018) provide estimates for the HN-GARCH model alongside the MLEs used for the IG-GARCH, reported in Table 2. Figure 9 uses these estimates in both cases. The behaviour of the two optimal strategies with respect to time seems almost identical, with the Gaussian approach yielding larger fractions of wealth invested in the risky asset in Figure 9(a) and the difference increasing as $\gamma \to 0$. It is very interesting to see that the relationship of the two solutions is reversed by changing the parameter setting to Set 2, plotted in Figure 9(b), even though the difference now is significantly smaller. One potential explanation refers to the different values for η directly affecting the skewness of the distribution of log asset return innovations. As displayed in Table 1, $|\eta_{2006}| > |\eta_{2018}|$, implying more left-skewness and excess kurtosis in the earlier parameter setting.[8] This, in return, coincides with less money invested in the risky asset in the plot in Figure 9 for the IG-GARCH solution, whereas the HN-GARCH model is not designed for capturing changes of this kind.

Table 3. Realized return moments for the three evaluated strategies, based on 1×10^4 simulation runs with 1×10^3 paths each, and expected utility from terminal wealth, obtained via the closed-form expressions.

	Panel A				Panel B
Solution	Mean	Std. dev.	Skewness	Kurtosis	$\phi_0(w_0, h_1)$
IG-GARCH	0.1678	0.2047	−0.4379	0.3785	−0.8635
HN-GARCH	0.1772	0.2548	−0.4393	0.3799	−0.8659
Merton	0.1804	0.2759	−0.4390	0.3791	−0.8683

Notes: The time horizon is $T = 252$, the parameters for both the IG-GARCH and the HN-GARCH solution are taken from Christoffersen, Heston, and Jacobs (2006).

The three strategies are now evaluated based on the values of the expected utility from terminal wealth, which is available in closed form. For a one-year time horizon, the parameter estimates from Set 1 and our standard choices for the investment parameters γ, ν_0 and r, Panel B in Table 3 reports the values of $\phi_0(w_0, h_1)$ for the three strategies. For these calculations, we set h_1 to match the unconditional variance of the IG-GARCH in the estimation. Note that fitting a homoskedastic Gaussian model to the underlying market data of Set 1 leads to a market price of risk of $\lambda_M = 3.106$, which is used in the formula of Merton's static solution, $\pi_t^M = \pi^M = (\lambda_M + 1/2)/(1 - \gamma)$.

Comparing the values, we can see that the highest expected utility is obtained with the IG-GARCH solution, as expected. It is to be expected that the second best choice among the three strategies is the one corresponding to the Gaussian GARCH model, outperforming the static solution.

We continue with an investigation of the return moments achieved by the three strategies, based on 10000 simulation runs with 1000 paths each. The results are presented in Panel A of Table 3. In this context, we note that for a five-years horizon and $\gamma = -1$, the IG-GARCH solution yields the smallest fraction of wealth invested in the risky asset, with $\pi_0^* \approx 1.35$. While an investor following the HN-GARCH would find $\pi_0^{HN} \approx 1.67$, Merton's static solution even suggests $\pi^M \approx 1.80$, which explains the higher mean return of the HN-GARCH strategy and Merton's solution, subject to higher volatility.[9] These differences are significant, i.e., standard errors are low for the first two moments. Obtaining similarly exact values for higher moments would be time-consuming with a large amount of simulations. The results for the alternative parameter estimates in IG and HN Set 2 are reported in Appendix A.1.3.

For the second part of this subsection, we analyse the parameter sensitivity of the wealth-equivalent loss, again based on a comparison of the optimal strategy to the HN-GARCH solution and to Merton's approach. Figure 10 describes WEL as a function of the level of risk aversion, using the parameter estimates from Set 1. We observe that for low levels of risk aversion, there is a difference of up to 2.5% of initial wealth between the HN-GARCH model and our optimal solution, which even increases up to 5% for Merton's static solution. The losses for both suboptimal strategies are decreasing in risk aversion. Extending the investment horizon can increase the losses dramatically, e.g., repeating the same analysis as in Figure 10 for a 20-years period yields around 8% WEL for the HN-GARCH and even up to 20% for Merton's solution, assuming low-risk aversion for the investor. For the alternative set of parameter estimates (Set 2), the performance of the Gaussian model is improved, see Appendix A.1.3.

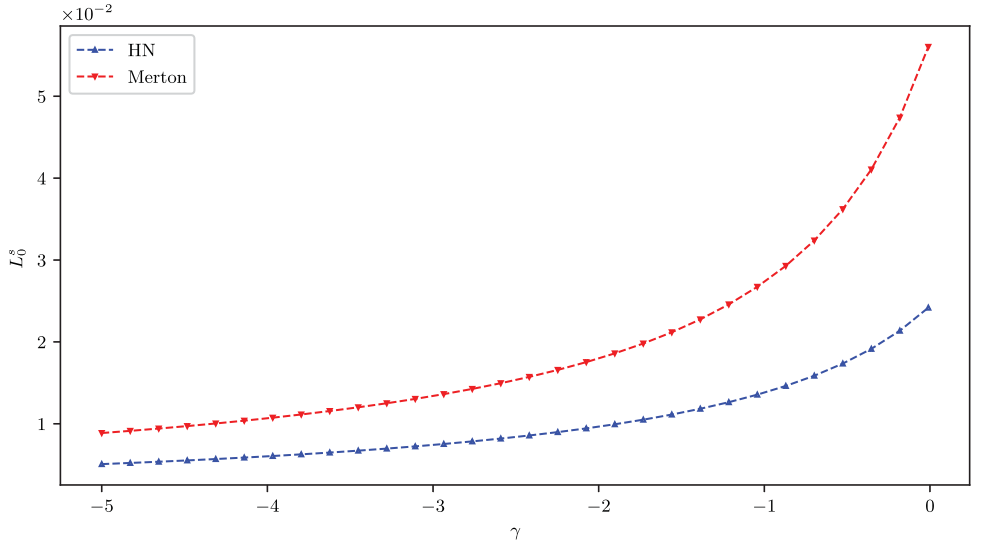

Figure 10. Dependence of L_0^s on the level of risk aversion γ for the HN-GARCH model and Merton's solution. The time horizon is five years with 252 trading days per year, the plots show $\gamma \in [-5, -0.01]$. This plot uses IG Set 1 (see Table 1) and the corresponding estimates for the HN-GARCH (see Table 2).

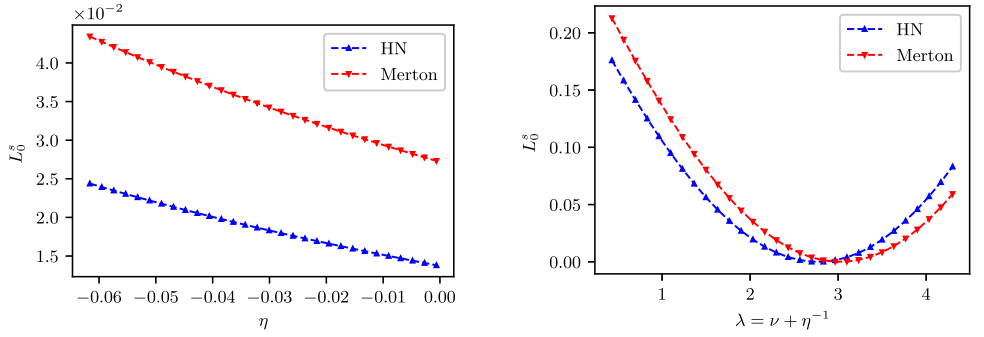

Figure 11. Dependence of L_0^s on η (Figure 11(a)) and the market price of risk (Figure 11(b)), respectively. The time horizon is five years with 252 trading days per year. The plot in Figure 11(a) captures influence of skewness and kurtosis of log asset returns with $\eta \in [-6.162 \times 10^{-2}, -6.162 \times 10^{-4}]$. Figure 11(b) displays sensitivity w.r.t. to the market price of risk in the interval $\lambda \in [0.5, 4.0]$. We use IG and HN Set 1 in both plots. (a) WEL dependent on η. (b) WEL dependent on λ.

For the plot in Figure 11(a), we use again the *combined approach* from Section 5.2 for the parameters of the IG-GARCH model in order to keep the first two moments constant and only change skewness and excess kurtosis as we move η. Note that the IG-GARCH and the Gaussian model calibrated with the estimates from the sources (see Tables 1 and 2) do not exactly match w.r.t. the first two moments. As stated above, Merton's solution is calculated with the risk premium derived from fitting a homoskedastic Gaussian model to the same market data. Figure 11(a) displays the impact of η on WEL for Set 1, i.e., the effect of skewness and kurtosis of one-step log return innovations. Since the IG-GARCH is set to

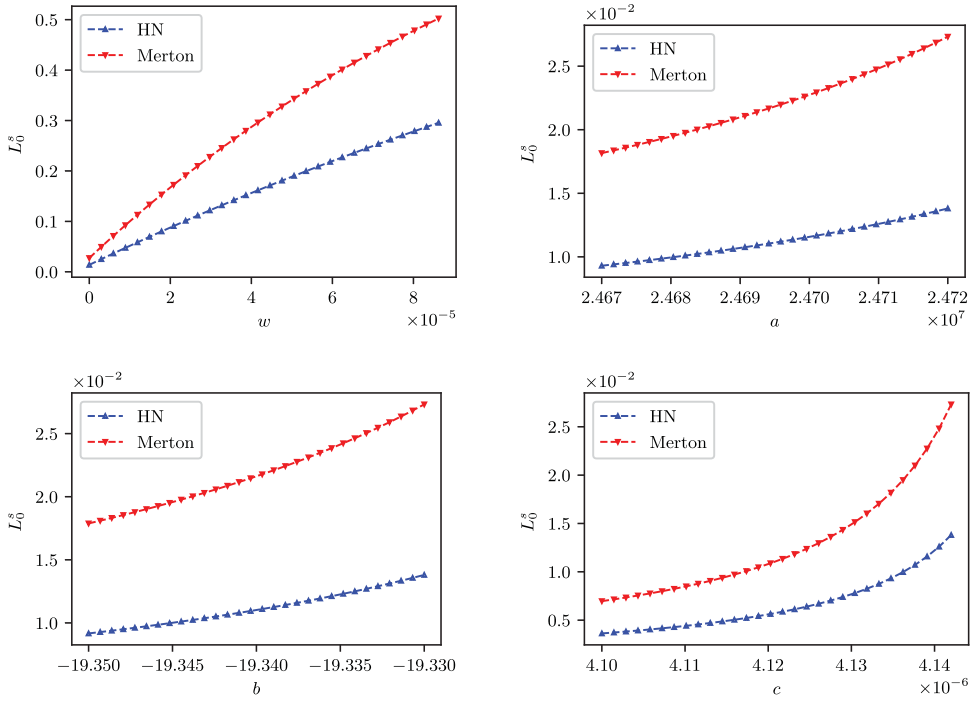

Figure 12. Dependence of L_0^s on w, a, b and c, respectively, plotted both for the HN-GARCH model and Merton's solution. The time horizon is $T = 5 \cdot 252$, the original parameter estimates are taken from Set 1.

model left-skewed log returns, one can clearly detect increasing losses of the HN-GARCH solution as the innovations become more negatively skewed for decreasing η. In this situation, with $\gamma = -1$, WEL could go up to 2.5% for the HN suboptimal choice, and even up to more that 4% for a Merton allocation, moving to $\eta = -0.06$. For the corresponding values of skewness and excess kurtosis of log asset returns in this context, see Figure 6(b). Figure 11(b) investigates the impact of the market price of risk on WEL. As before, the parameter settings for the HN-GARCH and the homoskedastic Gaussian model are not adapted when moving in the underlying grid, yielding clear increases in WEL for changes of λ in both directions. It is remarkable that for increases in the market price of risk, Merton's solution outperforms the Gaussian GARCH model. Remember in this context, that Merton's solution suggested the highest fraction invested in the risky asset, and therefore might cope better with higher risk premiums.

The analysis of the remaining parameters (w, a, b, c) with Set 1 is presented in Figure 12. The top left plot shows the intersection of the confidence interval for the MLE for w and $[0, \infty)$, in case of the other three parameters we only consider decreases from the original estimate to make sure the convergence condition is still satisfied (see the argumentation in Section 5.2). Increasing the parameter w yields the highest WEL, up to 30% for the HN-GARCH and even up to 50% for Merton's solution at the upper end of the confidence interval. Taking this into account, the losses seem vanishingly small for $w = 0$. For the parameters a, b and c, the plots in Figure 12 show a similar picture: A decrease in the parameter value leads to a decrease in WEL. As expected, Merton's solution is

outperformed by the dynamic HN-GARCH in all four cases. The plots for Set 2 can be found in Appendix A.1.3.

6. Conclusion

In this paper, we find an approximate closed-form representation to a portfolio optimization problem with one risky asset, whose log return follows a general affine GARCH process allowing for non-Gaussian innovations. The investor maximizes a CRRA utility from terminal wealth. Using a second-order approximation for the self-financing condition supported in the literature, we apply Bellman's principle iteratively to obtain the optimal strategy in recursive form. The optimal wealth process is shown to follow an affine GARCH process as well.

We develop one special case of our main result, the IG-GARCH model, which constitutes the first EUT closed-form solution available in the literature for a non-Gaussian GARCH model. Our solution also is a generalization of a recent result on HN-GARCH (a.k.a. Gaussian) models. One outstanding advantage of the new model is that asset returns follow a leptokurtic, negatively skewed distribution, allowing us to explore the impact of these non-Gaussian features on portfolio allocation.

Using two different sets of parameter estimates for the models, we investigate the performance of our investment strategy numerically. We address the feasibility of the portfolio problem, the quality of the SFC approximation, the sensitivity of the optimal solution to IG-GARCH and investment parameters, and report on an explicit comparison to the HN-GARCH model.

In particular, our analysis shows that for the prevailing sets of parameter estimates, we have a unique real solution to the optimality equation, maximizing CRRA utility. The effect of the second-order SFC approximation is negligible. Our special focus in the context of parameter sensitivity of our solution is on the impact of changes in higher return moments on the optimal strategies, where our results suggest that big shifts can change the optimal strategy significantly, also dependent on the investor's level of risk aversion. Calculations concerning the wealth-equivalent loss from following suboptimal strategies, particularly the HN-GARCH and Merton's static solution, indicate that an investor following the Gaussian strategy instead could face a loss of up to 2.5% with low-risk aversion. The loss could even increase up to 5% in case of choosing Merton's static solution. These outcomes suggest a significant impact of accommodating the fact that asset returns are negatively skewed and leptokurtic in a non-Gaussian GARCH modelling approach as compared to the already existing solutions.

It can be shown that a natural extension towards allowing for consumption using CRRA power utility functions is not solvable via Bellman's value iteration. Finding a setting where the investor derives utility not only from terminal wealth, but also from consumption at intermediate time points, thus remains an interesting open question.

Notes

1. It is possible to derive a set of HN-GARCH parameters matching the first two moments of a given IG-GARCH parameter set (Christoffersen, Heston, and Jacobs 2006). For this pair of models, the market price of risk in the IG-GARCH coincides with the parameter λ of the HN-GARCH model in (15a).

2. It is known (Escobar-Anel, Gollart, and Zagst 2022) that the optimal strategy in the HN-GARCH model converges to the continuous-time Heston solution as of Kraft (2005) for $\Delta \to 0$ under certain conditions. Thus, imposing these requirements and taking the limit $\eta \to 0$, our optimal solution approaches the continuous-time Heston strategy.
3. The same conclusions are obtained with the ML estimates from IG Set 2.
4. Note that the conclusion for the alternative set of parameter estimates from IG Set 2 is different, replicating the finding by Escobar-Anel, Gollart, and Zagst (2022) in the HN-GARCH framework. In these settings, however, the fraction of wealth invested in the risky asset is significantly smaller.
5. Note that the parameter λ of this artificial HN-GARCH calibration coincides with the market price of risk $\lambda = \nu + \eta^{-1}$ of the IG-GARCH. The notation thus is consistent.
6. Neither Equation (25) nor the recursive formula for $E^*_{t,T}$ depend on r or w.
7. The same if true for the relation of IG Set 2 and HN Set 2, of course.
8. The annualized volatility is even higher in the estimation in IG Set 2, suggesting that the effect of η on the conditional skewness is really propagated via the formula $\mathcal{S}_t[X_{t+1} - X_t] = 3\eta(h_{t+1})^{-1/2}$.
9. Note that the opposite is true for the alternative parameter set (see Appendix A.1.3), where the IG-GARCH suggests the largest fraction invested in the risky asset, followed by the HN-GARCH. This also coincides with a reversed order concerning realized return moments.
10. In contrast to the setting before, the estimate for w is now negative. We note that this can lead to negative values for the conditional variance in case the previous value is close enough to zero. Referring to Christoffersen, Heston, and Jacobs (2013), we adjust our parameter setting by imposing $w = 0$.
11. Indeed, $w < 0$ can be problematic w.r.t. the positivity of the conditional variance. We one more refer to Christoffersen, Heston, and Jacobs (2013) and the adjustment $w = 0$.

Disclosure statement

No potential conflict of interest was reported by the author(s).

ORCID

Marcos Escobar-Anel http://orcid.org/0000-0001-9691-4322

References

Babaoğlu Kadir, Peter Christoffersen, Steven L. Heston, and Kris Jacobs. 2018. "Option Valuation with Volatility Components, Fat Tails, and Nonmonotonic Pricing Kernels." *Review of Asset Pricing Studies* 8 (2): 183–231.

Badescu, Alexandru, Zhenyu Cui, and Juan-Pablo Ortega. 2019. "Closed-form Variance Swap Prices under General Affine GARCH Models and Their Continuous-time Limits." *Annals of Operations Research* 282 (1–2): 27–57.

Black, Fischer, and Myron Scholes. 1973. "The Pricing of Options and Corporate Liabilities." *The Journal of Political Economy* 81 (3): 637–654.

Bollerslev, Tim. 1986. "Generalized Autoregressive Conditional Heteroskedasticity." *Journal of Econometrics* 31 (3): 307–327.

Campbell, John Y., and Luis M. Viceira. 1999. "Consumption and Portfolio Decisions when Expected Returns are Time Varying." *Quarterly Journal of Economics* 114 (2): 433–495.

Christoffersen, Peter, Steven L. Heston, and Kris Jacobs. 2006. "Option Valuation with Conditional Skewness." *Journal of Econometrics* 131 (1–2): 253–284.

Christoffersen, Peter, Steven L. Heston, and Kris Jacobs. 2013. "Capturing Option Anomalies with a Variance-dependent Pricing Kernel." *Review of Financial Studies* 26 (8): 1963–2006.

Engle, Robert F. 1982. "Autoregressive Conditional Heteroscedasticity with Estimates of the Variance of United Kingdom Inflation." *Econometrica* 50 (4): 987–1007.

Escobar, Marcos, Sebastian Ferrando, and Alexey Rubtsov. 2015. "Robust Portfolio Choice with Derivative Trading under Stochastic Volatility." *Journal of Banking and Finance* 61: 142–157.
Escobar-Anel Marcos, Maximilian Gollart, and Rudi Zagst. 2022. "Closed-form Portfolio Optimization under GARCH Models." *Operations Research Perspectives* 9: 100216.
Heston, Steven L. 1993. "A Closed-form Solution for Options with Stochastic Volatility with Applications to Bond and Currency Options." *The Review of Financial Studies* 6 (2): 327–343.
Heston, Steven L., and Saikat Nandi. 2000. "A Closed-form GARCH Option Valuation Model." *Review of Financial Studies* 13 (3): 585–625.
Kraft, Holger. 2005. "Optimal Portfolios and Heston's Stochastic Volatility Model: An Explicit Solution for Power Utility." *Quantitative Finance* 5 (3): 303–313.
Merton, Robert C. 1969. "Lifetime Portfolio Selection under Uncertainty: The Continuous-time Case." *The Review of Economics and Statistics* 51 (3): 247–257.
Merton, Robert C. 1973. "Theory of Rational Option Pricing." *The Bell Journal of Economics and Management Science* 4: 141–183.
Mossin, Jan. 1968. "Optimal Multiperiod Portfolio Policies." *The Journal of Business* 41 (2): 215–229.
Ornthanalai, Chayawat. 2014. "Lévy Jump Risk: Evidence from Options and Returns." *Journal of Financial Economics* 112 (1): 69–90.
Samuelson, Paul A. 1969. "Lifetime Portfolio Selection By Dynamic Stochastic Programming." *The Review of Economics and Statistics* 51 (3): 239–246.

Appendix. Complementary Material

A.1 Alternative Parametric Choice

A.1.1 Feasibility of Solution and Approximation

Performing the above analysis concerning the quality of the approximation of the self-financing condition using the more recent ML estimates from Babaoğlu et al. (2018) (IG Set 2), we make the adjustment of setting $w = 0$.[10] In this adapted parameter setting, we obtain a very similar picture (see Figure A1) to the one described for IG Set 1. As before, the probability of the difference between V_T and e^{W_T} relative to the level of wealth V_T is centred around zero. The range is now slightly wider, but very close to the one observed in Figure 2 – the probability of the absolute value of the difference being less than 0.3% of the terminal wealth is close to one. Figure A2(a) shows a different picture than the equivalent plot w.r.t. to IG Set 1, see Figure 3. Note that with IG Set 2, assuming the same level of risk aversion, the fraction of wealth invested in the risky asset in significantly smaller – in particular, the share is between 0 and 1. Figure A2 replicates the finding from the corresponding analysis in the HN-GARCH environment, see Escobar-Anel, Gollart, and Zagst (2022). Concerning the accumulated amount of extra cash needed to account for the fact that the optimal strategy is not self-financing, Figure A2(b) suggests that putting aside 0.4% of the initial wealth in the beginning should cover all extra cash flows over the five-years time horizon under investigation.

A.1.2 Parameter Sensitivity

Concerning parameter sensitivity under the alternative IG Set 2, we first investigate the non-Gaussian behaviour, i.e., the impact of changes in η while keeping first and second order moments constant (see Section 5.2). As for IG Set 1, the plots in Figure A3 show that the fraction of wealth invested in the risky asset decreases as η decreases, i.e., as log asset returns become more skew and have a higher excess kurtosis. Again, referring to the colour bar in Figure A3(b), we note that the plotted range for η yields very extreme values for skewness and excess kurtosis at its lower end and is chosen for illustrative purposes. Figure A3(a) shows how the optimal initial solution depends on η for different levels of risk aversion, expressed via the parameter γ. The plot in Figure A3(b) isolates the dependency of the optimal solution on skewness and kurtosis. The IG-GARCH solution changes with respect to the parameter η, again showing a less risky allocation as η decreases.

An analysis of the impact of the market price of risk on the optimal strategy for the alternative parameter setting basically yields the same findings as presented in Figure 7. Again, an increase in the

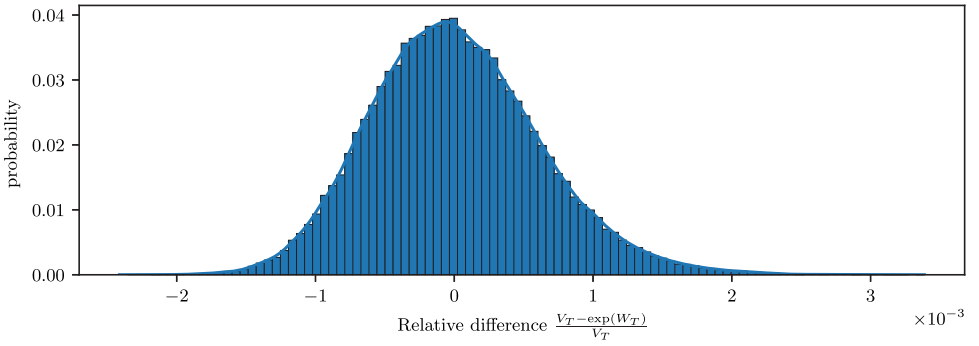

Figure A1. Comparison of the two wealth processes at time $T = 5 \cdot 252$, using IG Set 2 with $w = 0$.

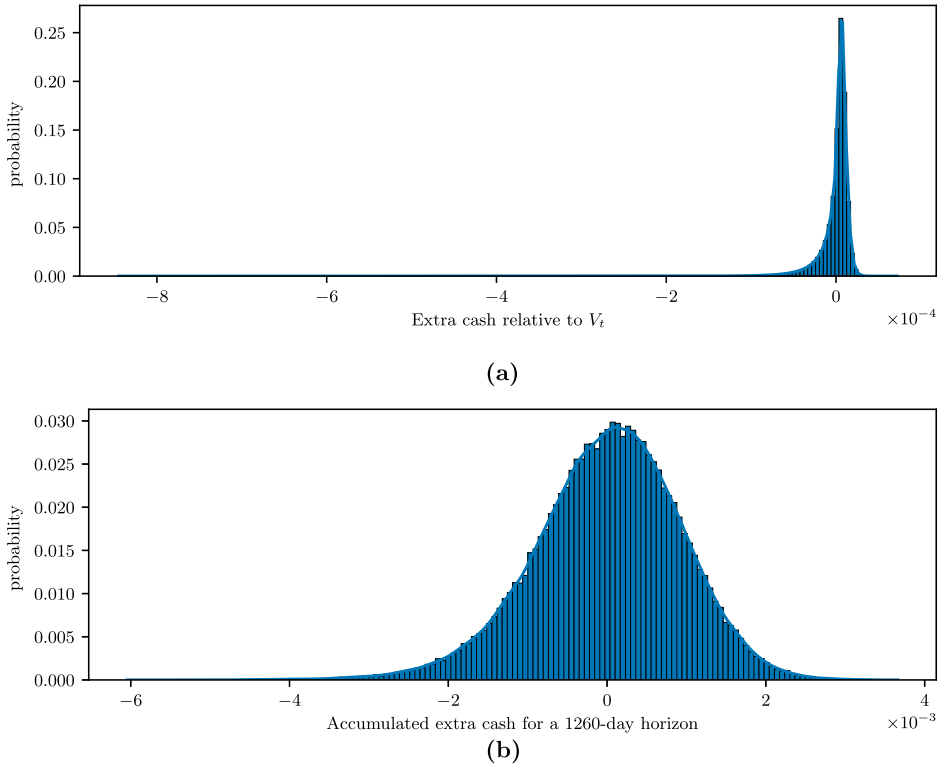

Figure A2. Extra cash needed for setting $V_t = e^{W_t}$ in each iteration over a five-years time horizon, using IG Set 2. (a) Histogram of adjustments in all simulations, over the whole time horizon. (b) Histogram of the accumulated amount of extra cash needed over the whole time horizon.

market price of risk leads to higher fractions of wealth invested in the risky asset, see Figure A4. Note however, as seen in other plots as well, that the general level of π_t^* is lower for this set of estimates.

Finally, also the sensitivity of the optimal strategy with respect to the parameters a, b and c shows a similar picture, as presented in Figure A5. We note that due to the larger standard errors for these estimates, the plotted range for the parameters is relatively large. The plots only show decreases in the parameters, starting from the original maximum likelihood estimate. Again, the limit of π_0^* as

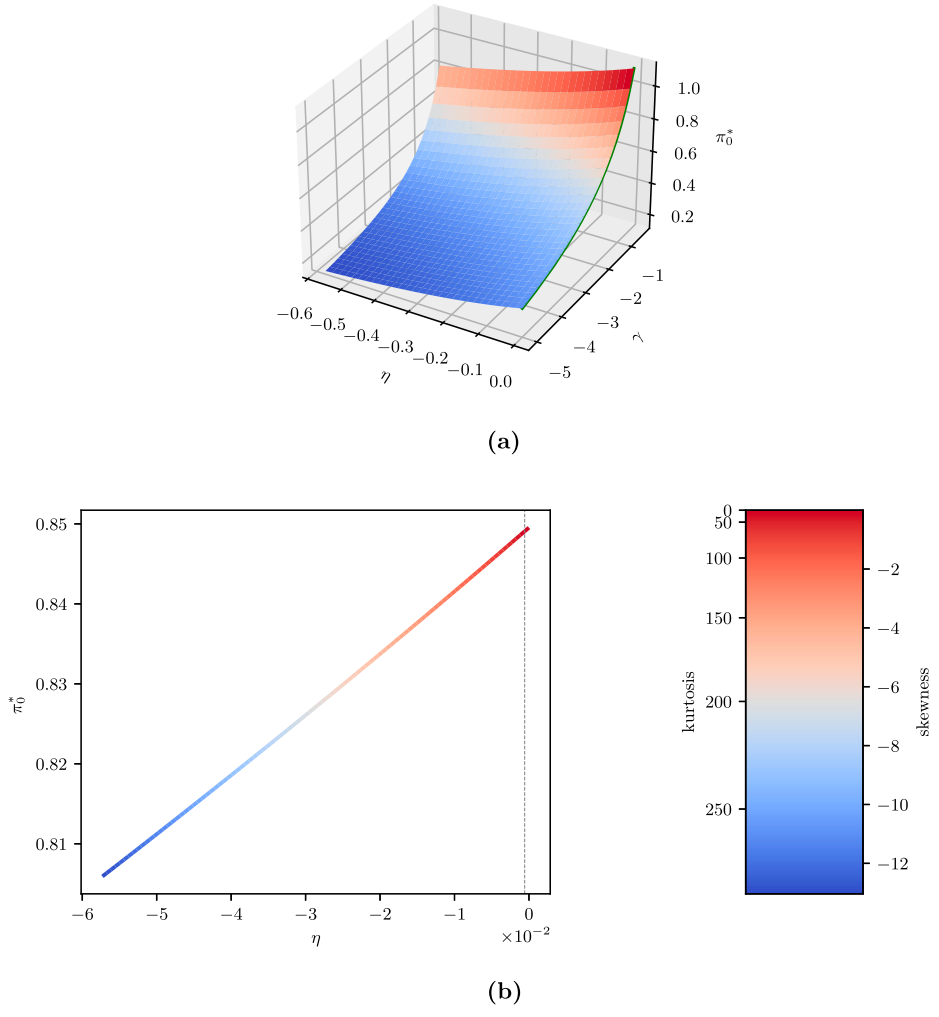

Figure A3. Dependence of π_0^* on γ and η (Part A3(a)) and on η alone (Part A3(b)) for a one-year time horizon. The prevailing parameter estimates are from IG Set 2 (see Table 1). (a) π_0^* dependent on γ and η. The x-axis scales the original estimate for η by a factor of at most 1×10^3, the range for γ is $[-5, -0.5]$. (b) π_0^* dependent on η only, with $\gamma = -1$. Here, η is scaled by at most 1×10^2. The colour bar indicates the corresponding values of skewness and kurtosis of the distribution of log asset return innovations.

a, b or c decrease turns out to be the value of the terminal solution – suggesting once more that the curve in Figure 4 is flattened. None of these parameters has any impact on the terminal solution.

A.1.3 Wealth-Equivalent Losses

Panel A of Table A1 shows the simulation results with respect to the return moments of the IG-GARCH strategy and the two alternatives – the Gaussian HN-GARCH strategy and Merton's static solution – in case of IG Set 2. As described in Section 5.3, Merton's solution is derived from a homoskedastic Gaussian model fitted to the same data set as IG and HN Set 2. In particular, this yields $\lambda_M = 0.78$ in this case. For this set of parameter estimates, the fraction of wealth invested in the risky asset is the largest for the IG-GARCH and lowest for Merton's strategy, which is remarkable since it shows the reversed order observed with the other parameter set. The new order justifies

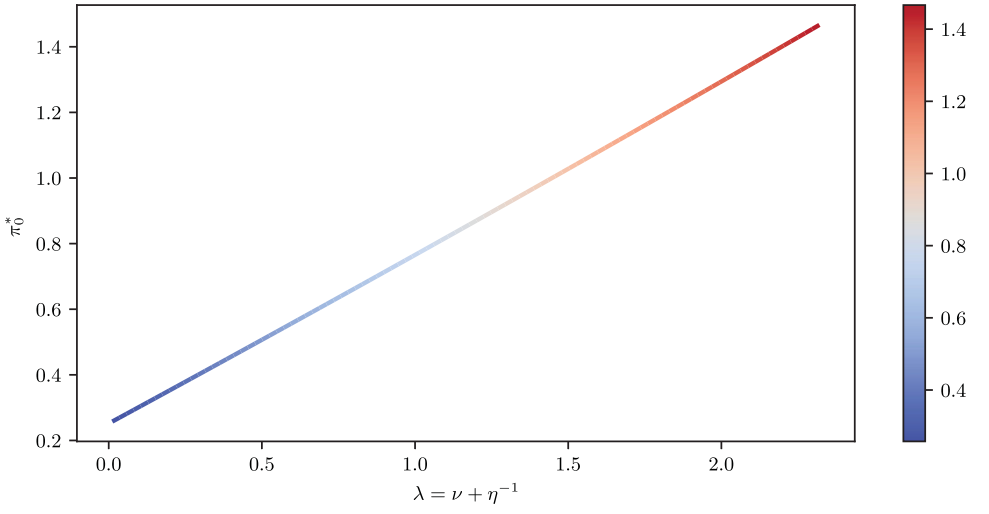

Figure A4. Dependence of π_0^* on the market price of risk for a one-year time horizon, original parameter estimates from IG Set 2. The value of the optimal initial solution increases significantly with λ.

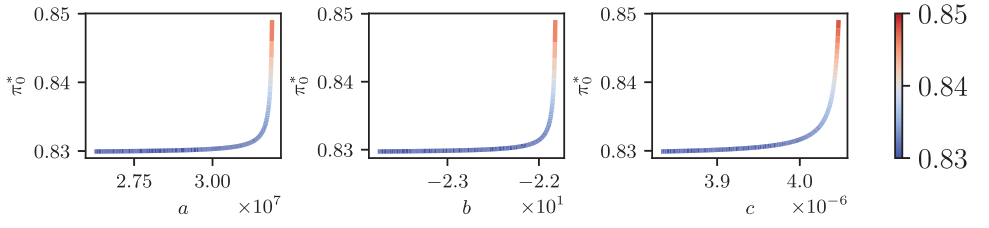

Figure A5. Dependence of π_0^* on a, b and c, respectively. The time horizon is $T = 252$, the original parameter estimates are taken from IG Set 2.

Table A1. Realized return moments for the three evaluated strategies, based on 1×10^4 simulation runs with 1×10^3 paths each.

	Panel A				Panel B
Solution	Mean	Std. dev.	Skewness	Kurtosis	$\phi_0(w_0, h_1)$
IG-GARCH	0.1424	0.1611	−0.6308	0.7064	−0.888227
HN-GARCH	0.1413	0.1551	−0.6306	0.7061	−0.888249
Merton	0.1347	0.1213	−0.6284	0.7024	−0.889204

Notes: The time horizon is $T = 252$, the parameters for both the IG-GARCH and the HN-GARCH solution are taken from Set 2.

the results presented in Panel A, with the optimal strategy yielding the highest mean return, subject to the largest volatility. As in Table 3, these differences w.r.t. the first two moments are significant. In terms of expected utility from terminal wealth, obtained via the closed-form expressions and reported in Panel B of Table A1, we note that the HN-GARCH solution keeps up with the optimal strategy quite well, taking into account in this context also the relatively small difference in allocation for the prevailing level of risk aversion.

Figure 10 again describes WEL as a function of the level of risk aversion, now for Set 2. The shape of the displayed curve is very similar to Figure 10, losses increase as risk aversion decreases. In general, due to the smaller difference between IG and HN allocation with the estimates from Set 2, losses are on a lower level. Since the performance of Merton's solution is inferior in this case, the

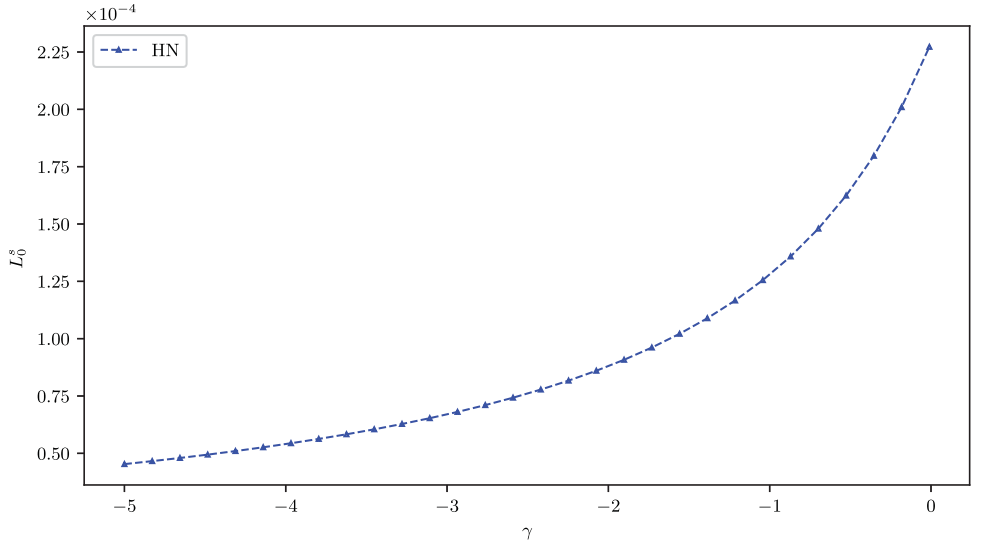

Figure A6. Dependence of L_0^s on the level of risk aversion γ for the HN-GARCH model. The time horizon is five years with 252 trading days per year, the plots show $\gamma \in [-5, -0.01]$. This plot uses IG Set 2 (see Table 1) and the corresponding estimates for the HN-GARCH (HN Set 2, see Table 2).

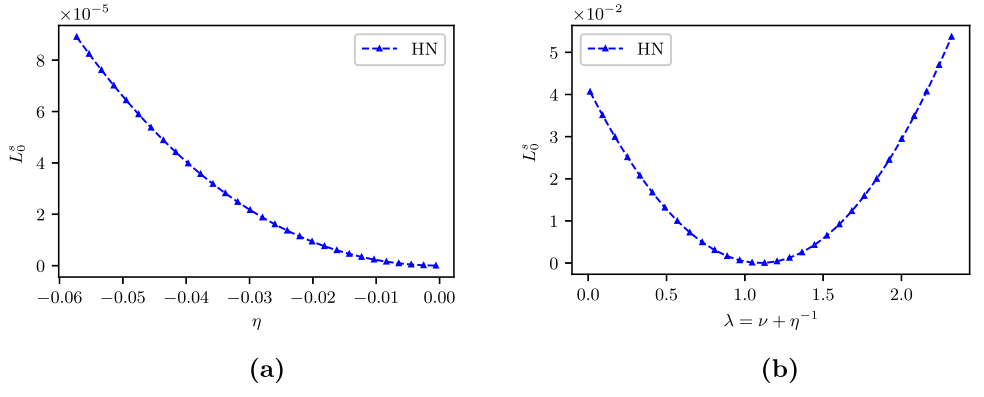

Figure A7. Dependence of L_0^s on η (Figure A7(a)) and ν (Figure A7(b)), respectively. The time horizon is five years with 252 trading days per year. The plot in Figure A7(a) refers to skewness and kurtosis of log asset returns and shows $\eta \in [-5.729 \times 10^{-2}, -5.729 \times 10^{-4}]$. Figure A7(b) displays sensitivity w.r.t. to the market price of risk in the interval $\lambda \in [0, 2.5]$. We use Set 2 in both plots. (a) WEL dependent on η. (b) WEL dependent on ν.

corresponding curve would prevent a detailed comparison of the GARCH models and is not shown in the plot.

For the remaining evaluation of the parameter sensitivity of the WEL under Set 2, we take a slightly different approach than for Set 1 in Section 5.3. Figure 9(b) shows that in this case, when working with the estimates for both GARCH models, the IG-GARCH yields a slightly higher fraction of wealth invested in the risky asset. To make differences more visible, we thus replace the MLE estimates for the HN-GARCH model from Babaoğlu et al. (2018) by an artificial set, derived directly

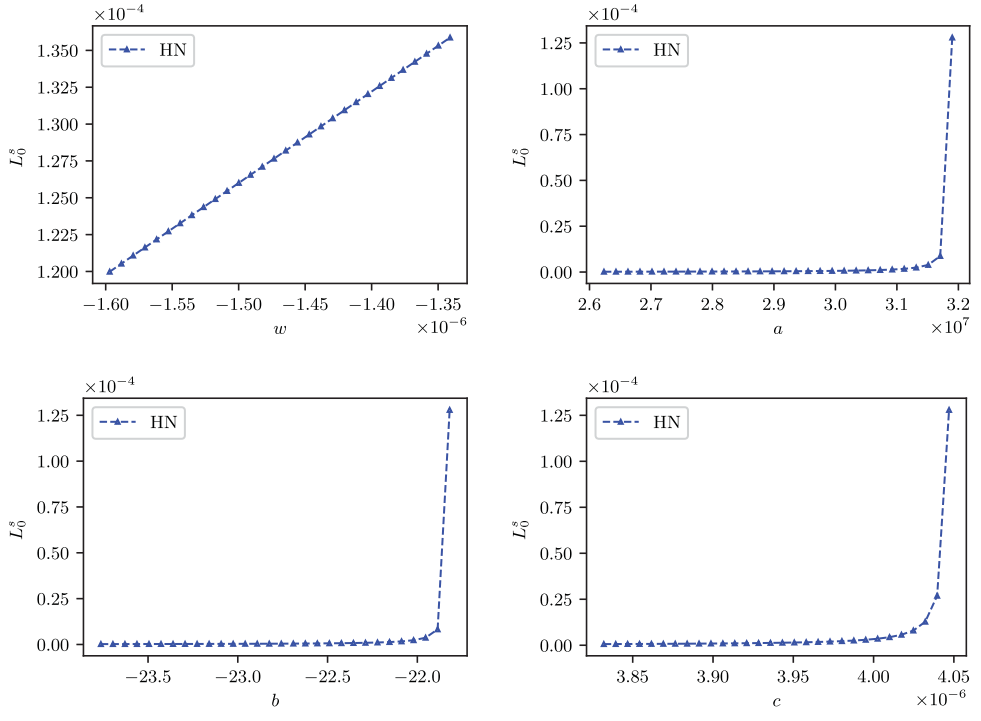

Figure A8. Dependence of L_0^s on *w*, *a*, *b* and *c*, respectively, plotted only for the HN-Model. In all cases, losses decrease, as the parameter is decreased. The time horizon is $T = 252$, the original parameter estimates are taken from Set 2.

from the IG-GARCH MLEs to match the first two moments. This approach implies an inferior performance of Merton's static solution, hiding the exact evolution of the HN-GARCH curves if plotted together. Therefore, this alternative is excluded from the following figures.

The plot in Figure A7(a), again created with the *combined approach* from Section 5.2 for the parameters of the IG-GARCH model, shows the dependency of WEL on η. The shape of the curve clearly suggests increasing losses of the HN-GARCH model as skewness increases and excess kurtosis decreases, respectively. Figure A7(b) investigates the impact of the market price of risk on WEL. As before, the HN-parameter setting is not adapted when moving in the underlying grid, yielding clear increases of WEL for changes of λ in both directions.

Figure A8 shows the plots of the wealth-equivalent loss for the remaining parameters *w*, *a*, *b*, and *c* of the model, in case of the alternative set of parameter estimates in Set 2. The top left plot shows the entire confidence interval for the MLE for *w*, in case of the other three parameters we only consider decreases from the original estimate to make sure the convergence condition is still satisfied. All four plots only show the HN-GARCH solution – including the not equally well performing Merton solution would prevent a detailed comparison of the two GARCH models. The plot for *w* suggests that the performance of the IG-GARCH can be improved w.r.t. its Gaussian counterpart by increasing the parameter. The curves for *a*, *b* and *c* are very similar to each other. As for Set 1 before (see Figure 12), decreases in these parameters let the WEL decrease, where the drop seems to be slightly slower for parameter *c*. In comparison to Figure 12, note that the confidence intervals for the MLEs are much larger now, revealing a larger section of the curve than for Set 1.